University of Mississippi

eGrove

Electronic Theses and Dissertations | Graduate School

1-1-2014

Investigating the photosynthesis of Symbiodinium in Caribbean gorgonian corals

Blake Ramsby
University of Mississippi

Follow this and additional works at: https://egrove.olemiss.edu/etd

 Part of the Ecology and Evolutionary Biology Commons

Recommended Citation

Ramsby, Blake, "Investigating the photosynthesis of Symbiodinium in Caribbean gorgonian corals" (2014). *Electronic Theses and Dissertations*. 1280.
https://egrove.olemiss.edu/etd/1280

This Dissertation is brought to you for free and open access by the Graduate School at eGrove. It has been accepted for inclusion in Electronic Theses and Dissertations by an authorized administrator of eGrove. For more information, please contact egrove@olemiss.edu.

INVESTIGATING THE PHOTOSYNTHESIS OF *SYMBIODINIUM* IN CARIBBEAN GORGONIAN CORALS

A Thesis

presented in partial fulfillment of requirements

for the degree of Master of Science

in the Department of Biology

The University of Mississippi

BLAKE D. RAMSBY

August 2014

Copyright Blake D. Ramsby 2014

ALL RIGHTS RESERVED

ABSTRACT

Symbiodinium photosynthesis fuels the growth of an array of marine invertebrates, including scleractinian corals and octocorals. Studies examining the symbiosis between Caribbean octocorals and *Symbiodinium* are sparse, even though octocorals blanket the landscape of Caribbean coral reefs. Here, I compared the photosynthetic characteristics of *Symbiodinium* in four common Caribbean octocoral species (*Pseudoplexaura porosa*, *Pseudoplexaura wagenaari*, *Eunicea tourneforti*, and *Pterogorgia anceps*) in outdoor aquaria at ambient temperature. The four octocoral species exhibited similar photochemical efficiencies despite significant differences in *Symbiodinium* density, chlorophyll *a* per cell, light absorption by chlorophyll *a,* and rates of photosynthetic oxygen evolution. Differences in photosynthetic performance between octocoral species could not be easily attributed to the physiology of either symbiotic partner, as the four octocoral species associated with one of three *Symbiodinium* internal transcribed spacer 2 (ITS2) types. *P. porosa* and *P. anceps* harbored the same *Symbiodinium* type but exhibited markedly different photosynthetic characteristics, which highlights the importance of host morphology on *Symbiodinium* performance.

I also compared the photosynthetic performance of *Symbiodinium* in discrete growth forms of *Briareum asbestinum* at ambient and at elevated temperature. *B. asbestinum* grows in either an encrusting or branching morphology, each of which co-occurs and associates with distinct *Symbiodinium* types (B19 in encrusting, B21 in branching). The two morphologies had different symbiotic characteristics at ambient temperature, as encrusting fragments had greater

Symbiodinium and chlorophyll densities cm^{-2}; however, photosynthetic oxygen evolution was not significantly different. In addition, branches had higher photochemical and light absorption efficiencies than encrusting fragments. At elevated temperature, more negative impacts were seen in branches than in encrusting fragments, including impaired photochemical efficiency and a decreased ratio of photosynthesis to respiration. Neither morphology exhibited coral bleaching at elevated temperature, despite negative effects of elevated temperature on photosynthesis by *Symbiodinium*. A decreased ratio of photosynthesis to respiration represents a potential fitness cost to branches, as the energetic contribution of their *Symbiodinium* may be reduced at elevated temperature. Understanding the symbioses between gorgonian corals and Symbiodinium and how they respond to elevated temperature will aid in understanding why gorgonian corals dominate many Caribbean reefs.

LIST OF ABBREVIATIONS AND SYMBOLS

α	initial slope of the photosynthesis-irradiance curve
β	photoinhibition coefficient
1-β	statistical power
$a^*_{\text{chl } a}$	chlorophyll *a* specific absorption coefficient
AIC	Akaike information criterion
ANOVA	analysis of variance
BIC	Bayesian information criterion
chl	chlorophyll
CTAB	cetrimonium bromide
$\Delta F/Fm'$	effective yield of photosystem II at solar noon
D_e	estimated absorbance
D_{e675}	estimated absorbance at 675 nm
$D_{e400\text{-}750}$	estimated absorbance spectrum from 400 to 750 nm
df	degrees of freedom
DGGE	denaturing gradient gel electrophoresis
DMSO	dimethyl sulfoxide
E_c	compensation irradiance
E_k	saturation irradiance
F	F statistic

Fv/*Fm*	maximum yield of photosystem II at dusk
ITS2	internal transcribed spacer region II of ribosomal DNA
MS	mean square
msh1	the mitochondrial DNA mismatch repair gene
n	sample size
P	photosynthetic rate of oxygen production (μmol O_2 hr^{-1})
P	statistical probability
P-E	photosynthesis versus irradiance
PAM	pulse amplitude-modulated fluorometer
PAR	photosynthetically available radiation
PCR	polymerase chain reaction
P_{max}	maximum gross rate of oxygen production
P_s	the maximum photosynthetic rate in the absence of photoinhibition
PSII	photosystem II
PVC	polyvinyl chloride
Q_m	pressure over photosystem II
ρ	pigment density of chlorophyll *a* (mg m_{-2})
R	respiration (rate of oxygen consumption; μmol O_2 hr^{-1})
r	effect size or the correlation coefficient
Sym	the dinoflagellate genus *Symbiodinium*
t	t statistic
Tukey HSD	Tukey honest significant difference

U	Mann-Whitney test statistic
χ^2	chi-squared statistic

ACKNOWLEDGEMENTS

I would like to thank my major advisor, Dr. Tamar Goulet for her efforts to make me a better scientist and for her guidance. I would like to thank Dr. Roberto Iglesias-Prieto for welcoming me into his lab and sharing his knowledge of photosynthesis. I am grateful to my committee members Drs. Stephen Brewer and Brice Noonan. S. Enríquez and A. Banaszak provided valuable support, suggestions, and insight. R. Smith, N. Schubert, D. Goulet, H. Pearson, L. Camp, and the staff and students of the Unidad Académica de Sistemas Arrecifales, Instituto de Ciencias del Mar y Limnología, Universidad Nacional Autónoma de México all made contributions to this work. I need to thank my fellow graduate students, K. Shirur, M. McCauley, B. Piculell, S. Nielsen, K. Byler, L. Carter, and J. Howell for putting up with my rants as well as my tantrums. This work would have never been completed without the blood, sweat, and friendship of K. Shirur. The University of Mississippi Biology Department and the Graduate School provided generous support for conference travel. This thesis was funded by grants from the Explorer's Club and the University of Mississippi Graduate Student Council. In addition, this material is based upon work supported by the National Science Foundation under Grant No. (IOS 0747205) to Tamar L. Goulet. Any opinions, findings, and conclusions or recommendations expressed in this material are those of the authors and do not necessarily reflect the views of the National Science Foundation.

TABLE OF CONTENTS

LIST OF TABLES

LIST OF FIGURES

INTRODUCTION

As animals, corals (Eukarya, Animalia, Cnidaria) obtain energy via heterotrophy, stinging prey with cnidocytes on the tentacles of their polyps (Houlbreque and Ferrier-Pages 2009; Ferrier-Pages et al. 2011). Many corals, including most tropical species, also can obtain energy via photoautotrophy, via a symbiosis with symbiotic dinoflagellates of the genus *Symbiodinium* ("zooxanthellae"), which use light energy to fix carbon (Warner et al. 2010; Dubinsky and Falkowski 2011). Thus, most tropical coral colonies – even a single coral polyp – represent a symbiosis of two very different organisms, an autotrophic alga and a heterotrophic animal.

Symbiodinium reside in the gastrodermal cells of corals, which reflects the intimacy of their symbiosis. In the gastroderm, *Symbiodinium* utilize the byproducts of coral metabolism, namely inorganic carbon (CO_2) for photosynthesis and nitrogenous wastes for protein and DNA synthesis (e.g., NH_3, NO_3^-, or N_2; Yellowlees et al. 2008). More than 30% of carbon fixed by *Symbiodinium* can be delivered to the host (Muscatine 1967; Muscatine and Cernichiari 1969).

The amount of carbon transferred to the host coral, as well as the physiology of the symbiosis, can be influenced by internal and external factors. Most coral species associate with one or a select few *Symbiodinium* taxa and do not readily associate with different *Symbiodinium* (Goulet 2006). *Symbiodinium* taxa vary in their physiological characteristics (Rowan 2004; Tchernov et al. 2004; Thornhill et al. 2008; Hennige et al. 2009), therefore the high specificity between host taxa and *Symbiodinium* couples coral and algal fitness (Day et al. 2008; Sampayo

et al. 2008). Symbiotic characteristics vary amongst different coral:*Symbiodinium* combinations, including the density (Fitt et al. 2000), light absorption (Jones and Berkelmans 2012), and photosynthetic oxygen production of *Symbiodinium* (Rowan 2004). From the perspective of *Symbiodinium*, association with a different coral host can affect its cellular density as well as its photosynthetic characteristics. Corals exhibit various morphologies and can grow in a flat, mounding, or branching morphology, resulting in a horizontal or vertical orientation of the host, which in turn affects the incident irradiance that the *Symbiodinium* can utilize for photosynthesis. Horizontal morphologies are exposed to more downwelling irradiance than vertical or branched morphologies (Warner and Berry-Lowe 2006), which may also experience self-shading within a colony. The thickness of coral tissue also impacts photosynthesis by *Symbiodinium*, as thicker coral tissue reduces the amount of light that reaches *Symbiodinium* cells (Kaniewska et al. 2011; Dimond et al. 2012) and limits their photosynthetic rate. Thus, the physical characteristics of different host species have complex effects on the photosynthesis by their endosymbionts.

In addition, external factors, such as nitrogen inputs (Borell and Bischof 2008), temperature changes (Rowan 2004), or light levels (Dubinsky et al. 1984; Gorbunov et al. 2001) can affect photosynthesis in a coral symbiosis. Temperature changes, in particular, can impair photosynthesis (Jones et al. 1998; Warner et al. 1999), which often precedes the dissociation of the symbiosis that occurs during coral bleaching (Brown 1997; Weis 2008).

This work explores the photosynthetic characteristics of *Symbiodinium* in symbiosis with gorgonian corals (Bayer 1961), which belong to the Anthozoan subclass Octocorallia and are abundant on Caribbean reefs (Ruzicka et al. 2013). In contrast to reef-building scleractinian corals (subclass Scleractinia), which form a thin veneer of tissue over calcium carbonate

substrate, gorgonian corals form branches composed of a thicker layer of tissue that encircles a central axis of microscopic calcium carbonate sclerites and protein. While some scleractinian corals also form branches, gorgonian colonies take on unique morphologies, often with long branch that split off of a central holdfast that is anchored to the reef.

Despite their abundance, Caribbean gorgonian species remain a an ecological black box, as we know little about how gorgonians obtain nutrition (e.g., heterotrophy and symbiotic autotrophy Burkholder and Burkholder 1960; Kanwisher and Wainwright 1967; Ribes et al. 1998), how they interact with other organisms on the reef (Vreeland and Lasker 1989), or how they will respond to future climate stressors (Drohan et al. 2005; Mydlarz and Jacobs 2006).

I. *SYMBIODINIUM* PHOTOSYNTHESIS IN CARIBBEAN OCTOCORALS

Introduction

Gorgonian corals (subclass Octocorallia) are abundant and important members of coral reef communities throughout the Caribbean (Cary 1918; Bayer 1961; Kinzie 1973; Lasker 1985; Lasker et al. 1988; Vreeland and Lasker 1989; Ruzicka et al. 2013). Unlike the dramatic decline of scleractinian corals in the Caribbean (Hughes 1994; Gardner et al. 2003; Pandolfi et al. 2005; Edmunds and Elahi 2007), gorgonian coral abundance is the same or even increasing (Miller et al. 2009; Colvard and Edmunds 2011; Ruzicka et al. 2013). For example, in the Florida Keys, gorgonian octocoral abundance increased significantly since 1999 (Ruzicka et al. 2013). And, in the US Virgin Islands, the abundance of two of three gorgonian species studied has increased since 1992 (Colvard and Edmunds 2011). Gorgonian corals are also abundant in the Yucatan coast of México, where gorgonian species richness can exceed scleractinian coral species richness (Dahlgren 1989).

Despite being prominent members of Caribbean reef communities, studies on gorgonian corals are sparse, predominantly focusing on the gorgonian coral hosts without addressing their symbiosis with the unicellular dinoflagellates in the genus *Symbiodinium*. Studies tracked digested material (Murdock 1978b,a), described sclerite formation (microscopic skeletal elements; Goldberg and Benayahu 1987a,b), or measured growth (Brazeau and Lasker 1992;

Lasker et al. 2003), and feeding rates (Lasker 1981; Ribes et al. 1998). In addition, gorgonian secondary metabolites have been extensively studied due to their medical and economic importance (reviewed in Rodríguez 1995). A few early studies measured the photosynthetic rates of *Symbiodinium* in Caribbean gorgonians (Burkholder and Burkholder 1960; Kanwisher and Wainwright 1967), while key photosynthetic characteristics, such as photochemical and light absorption efficiencies, have not been measured. Furthermore, the few studies that investigated the physiology of Caribbean gorgonian corals and their *Symbiodinium* did not identify the *Symbiodinium* present.

The genus *Symbiodinium* contains nine phylogenetic clades, A-I (Pochon and Gates 2010), although clade E may represent a single species (Jeong et al. 2014). Within each clade, *Symbiodinium* are often distinguished using sequences of the internal transcribed spacer regions of ribosomal DNA (*Symbiodinium* types sensu (LaJeunesse 2001)). Differences between *Symbiodinium* types can correlate with ecological (Sampayo et al. 2007; Finney et al. 2010) and physiological differences (e.g., Sampayo et al. 2008) between cnidarian hosts. Almost all Caribbean gorgonian species associate with *Symbiodinium* clade B types and many harbor type B1 (LaJeunesse 2002; Goulet et al. 2008). Within type B1, multiple lineages have been identified (Santos et al. 2004; Finney et al. 2010).

Collecting baseline physiological data on coral-algal symbioses (e.g., Imbs and Dautova 2008; Edmunds et al. 2011), and not just data when the symbioses are stressed, are critical to evaluating the effects of stressors on symbioses. The objective of this study was to characterize the photosynthesis of *Symbiodinium, in hospite* and in isolation, in four common Caribbean gorgonian species: *Pterogorgia anceps*, *Eunicea tourneforti*, *Pseudoplexaura porosa,* and

Pseudoplexaura wagenaari. Studying the physiology of the symbiosis between gorgonian corals and *Symbiodinium* may shed light on why gorgonian corals dominate Caribbean reefs while scleractinian coral abundance is declining.

Methods

Sample collection and acclimation

In June 2010, gorgonian branches were collected at 3 m depth from a patch reef near Puerto Morelos, Quintana Roo, México (20° 52' N, 86° 51' W). One branch was removed from each sampled colony of the four gorgonian species: *Pterogorgia anceps* (n=9), *Eunicea tourneforti* (n=9), *Pseudoplexaura porosa* (n=9), and *Pseudoplexaura wagenaari* (n=6). Branches were held in outdoor aquaria with flowing seawater for 11 days for acclimation. The temperature in the aquaria was 29.5 ± 0.5° C, similar to the ambient temperature on the reef. Light levels in the aquaria were maintained at levels similar to those at the collection site (~900 µmol quanta m^{-2} s^{-1} at solar noon) by shading the aquaria with window screening.

Photochemical efficiency of photosystem II in *Symbiodinium*

Throughout the acclimation period, the photochemical efficiency of photosystem II of the *Symbiodinium* in each branch was measured using a diving pulse amplitude modulated (PAM) fluorometer (WALZ, Effeltrich, Germany) at solar noon ($\Delta F/F_m'$; effective yield) and after sunset (F_v/F_m; maximum yield). Photochemical efficiency was measured approximately 2 cm below the branch tip at a constant distance from the surface of the branch. Using the effective and maximum yield values obtained for each species, we calculated the maximum excitation

pressure over photosystem II, Q_m, for each species, whereby $Q_m = 1-((\Delta F/F_m') / (F_v/F_m))$ (Iglesias-Prieto et al. 2004).

Oxygen flux of *Symbiodinium* in gorgonian branches

After 11 days of acclimation, the oxygen fluxes of the branches were measured using Clark-type oxygen electrodes in twin 0.5 l acrylic chambers. The electrodes were connected to a 782 Oxygen Meter (Strathkelvin Instruments Ltd., North Lanarkshire, Scotland). The chambers were filled with 0.45 µm filtered seawater with 4 mM sodium bicarbonate (e.g., Iglesias-Prieto and Trench 1994). Water was circulated inside each chamber using a small pump. Electrodes were calibrated by bubbling oxygen and nitrogen gas to define 100% and 0% oxygen concentrations, respectively. A water jacket, connected to a water recirculator, maintained the temperature of 29.0-29.5° C inside the chambers.

To measure the oxygen flux of a gorgonian branch, a branch was sealed in a chamber. Following a 20 min acclimation, respiration was measured for 10 min in darkness. Then, the branch was illuminated from one direction with three 6W LED light bulbs, while white acrylic on the sides and rear of the chamber reflected the light within the chamber. The branch was exposed to 11 irradiance levels (0-2200 µmol quanta m^{-2} s^{-1}) by progressively removing sheets of window screening. The irradiance levels in each chamber were measured using a 4π quantum sensor (WALZ, Effeltrich, Germany). A gorgonian branch was exposed to each irradiance level for up to 15 min, or until a linear change in oxygen concentration was recorded in the chamber. Following the last light level, respiration was measured again in darkness.

Oxygen flux measurements required 2.5 h per sample and were collected at approximately 09:00 or 12:00 local time. Due to the lengthy data collection time, it took 10 days to measure the

oxygen fluxes of all the gorgonian branches. To account for changes in photosynthetic rate at different times of day, the photosynthesis of *Symbiodinium* in each gorgonian species was measured at alternate times on consecutive days.

After measuring the oxygen flux, the surface areas of the gorgonian branches were calculated. For gorgonian species with cylindrical branches (*E. tourneforti*, *P. porosa*, and *P. wagenaari*), we measured the length and diameter of each branch and calculated the surface area of a cylinder. For *P. anceps,* whose branches are blade like, we measured the diameter and length of the blade and calculated the surface area by combining the areas of a series of rectangles.

Isolation and oxygen flux of isolated *Symbiodinium*

Branches were returned to shaded aquaria for 1 h before *Symbiodinium* isolation. *Symbiodinium* were isolated by homogenizing, in a mortar and pestle, a 2 cm section of the gorgonian branch, obtained 3 cm below the tip of the branch. The homogenate was diluted in 20 ml of 0.45 μm filtered seawater and centrifuged for 1 min at 500 rpm. The liquid fraction was filtered through 150, 74, and 20 μm nitex meshes. The filtered fraction was then centrifuged for 1 min at 3500 rpm and the *Symbiodinium* pellet was washed two times with 10 ml of filtered seawater. Following the last wash, the *Symbiodinium* pellet was resuspended in 5 ml of filtered seawater and divided into aliquots for oxygen flux measurements (0.5 ml), chlorophyll content (1.5 ml), cell density (0.25 ml), and genetic identification (2 ml).

To measure isolated *Symbiodinium* oxygen flux, 0.5 ml of the *Symbiodinium* slurry was mixed with 2.5 ml filtered seawater containing 4 mM $NaHCO_3$ and loaded into a water-jacketed glass cell respirometry chamber (StrathKelvin Instruments Ltd). The *Symbiodinium* samples were stirred with magnetic stir bars and maintained at 29° C with a water recirculator. Oxygen

flux measurements were recorded in two chambers simultaneously using Clark-type oxygen electrodes. Respiration was measured in darkness for 10 min before and after a series of irradiance levels. The isolated *Symbiodinium* were exposed to 13 increasing irradiance levels (0-2200 μmol quanta m^{-2} s^{-1}) for 10 minutes per level or until a linear change in oxygen concentration was observed in the chamber. For each sample, the irradiance levels were measured using a 4π quantum sensor (WALZ, Effeltrich, Germany). Oxygen fluxes of isolated *Symbiodinium* were measured after those of the intact branches, at approximately 15:00 or 16:00 local time.

Calculation of photosynthetic rates

Net and gross rates of oxygen flux were plotted against irradiance to generate photosynthesis versus irradiance (P-E) graphs. Coefficients from P-E curves (P_s, the maximum photosynthetic rate in the absence of photoinhibition; α, the initial slope of the curve; and β the photoinhibition coefficient) were determined for each sample by fitting the equation of Platt et al. (1980) using the nlsList function in the nlme package of the R statistical software. Photosynthetic rates were standardized to the surface area of the gorgonian branch, the total number of *Symbiodinium*, and the total amount of chlorophyll *a*. α was standardized to the amount of chlorophyll *a*. To calculate the diurnal balance between gross photosynthesis and respiration, we integrated the P-E curve over the irradiance for a 24 h period.

Symbiodinium density

Symbiodinium density in a gorgonian branch was estimated from averaging four replicate hemocytometer counts (0.4 mm^3 each) of the *Symbiodinium* cell density aliquot. Oxygen fluxes

of gorgonian branches were standardized to the total number of *Symbiodinium* cells in a branch, which was estimated using the density of cells in the homogenized piece (cells cm^{-2}) multiplied by the surface area of the entire branch. For isolated *Symbiodinium*, the number of cells in the respirometry chamber was estimated using the cell density determined from the *Symbiodinium* cell density aliquot.

Chlorophyll content in *Symbiodinium*

For chlorophyll quantification, the *Symbiodinium* cells in the 1.5 ml aliquot of the *Symbiodinium* slurry were pelleted, and the supernatant was decanted. Chlorophylls were extracted from the *Symbiodinium* cells by adding 950 µl of cold 100% acetone and 50 µl DMSO. After 24 h of extraction at -20 °C in the dark, the absorbance of the extract was measured at 630, 660, and 750 nm using an ELYPTICA model ELy-2000 spectrophotometer. Absorbance at 750 nm was subtracted from the absorbance at 630 nm and 660 nm for each sample and chlorophylls *a* and c_2 were estimated using the equations of Jeffrey and Humphrey (1975). Chlorophyll concentrations were standardized to surface area (µg chl cm^{-2}) and to cell density (pg chl $cell^{-1}$). Oxygen flux of gorgonian branches was standardized to the total amount of chlorophyll *a* in the gorgonian branches, which was calculated using the concentration of chlorophyll per surface area of the homogenized piece multiplied by the surface area of the entire branch. For isolated *Symbiodinium*, the amount of chlorophyll *a* in the respirometry chamber was estimated using the chlorophyll *a* concentration obtained from the 1.5 ml chlorophyll content aliquot.

Estimated absorbance and chlorophyll *a* specific absorption

Following the oxygen flux measurements, the reflectance spectrum (400-750 nm) of each branch was measured using an Ocean Optics USB 4000 fiber optic spectrophotometer. The fiber optic cable was held at a 45° angle above a branch, which was illuminated on all sides to produce a homogeneous light field (designed by T. Scheufen, UNAM). A dried gorgonian branch, painted with white acrylic paint, was used to correct for light scattered by the surface of the gorgonian branch. The painted branch reflected ~90% of PAR compared to a similarly shaped object wrapped in Teflon. Surface-corrected reflectance spectra were standardized to the reflectance value at 750 nm. Estimated absorbance spectra (D_e) were calculated as the negative log of the corrected reflectance. Chlorophyll *a* specific absorption ($a^*_{chl\ a}$), was calculated using the equation $a^*_{chl\ a} = (D_{e\ 675} / \rho) \times \ln(10)$, where ρ is mg m^{-2} of chlorophyll *a* (Enríquez et al. 2005).

Genetic identification of *Symbiodinium*

For each gorgonian branch, 2 ml of the isolated *Symbiodinium* slurry was centrifuged at 10,000 rpm for 1 min to pellet the *Symbiodinium* cells. The supernatant was removed and replaced with 2 ml 100% EtOH to preserve the *Symbiodinium*. DNA was extracted from an aliquot of this solution using the Qiagen DNeasy Plant Mini kit. The internal transcribed spacer 2 (ITS2) region of ribosomal DNA was amplified using the primers ITSintfor2, ITS-Reverse, and ITS2CLAMP following the protocol of LaJeunesse (2002). The PCR products were separated using denaturing gradient gel electrophoresis (DGGE) with a 45-80% denaturing gradient and run at 120 V for 13 h. Dominant ITS2 sequence variants in unique profiles were excised, re-

amplified using ITSintfor2 and ITS-Reverse, and then sequenced using an Applied Biosystems 3730XL automated sequencer at the DNA Laboratory at Arizona State University.

Since we found that at least one colony of each of the four gorgonian species harbored *Symbiodinium* type B1, we determined whether colonies of the four different species harbored the same B1 lineage (Finney et al. 2010). Microsatellite flanking regions from B1 *Symbiodinium* were PCR amplified with the primers B7Sym15 (Pettay and LaJeunesse 2007) and CA4.86 (Santos et al. 2004) and directly sequenced using an Applied Biosystems 3730XL automated sequencer at the DNA Laboratory at Arizona State University. The flanking sequences were concatenated and aligned with published *Symbiodinium* type B1 sequences (Supplementary table S1 in Finney et al. 2010; Thornhill et al. 2013). Six samples, five from our study (2 *P. porosa*, 2 *P. wagenaari*, 1 *P. anceps*) and one published (B1 lineage 1.4, Finney et al. 2010) were only represented by B7Sym15 sequences. For each flanking region, the Jukes Cantor model of sequence evolution was chosen using AIC scores from jModelTest (Posada 2008,2009) and substitution rates were assumed to follow a gamma distribution with four categories. In order to determine the phylogenetic relationships among B1 *Symbiodinium*, a Bayesian phylogenetic tree was generated using the MrBayes (Huelsenbeck and Ronquist 2001). Two sets of four independent chains were run for 1,000,000 generations, but the model converged after 916,000 generations. Trees were sampled every 100 generations (916 trees per run) and the first 25% of trees were discarded as burn-in. The average standard deviation of split frequencies was less than 0.01. To confirm the topology generated by MrBayes, 100 bootstrap replicates of a maximum-likelihood phylogenetic tree were generated in Garli 2.0 using the Jukes Cantor model of

sequence evolution (Zwickl 2006). *Symbiodinium* type B19 (Supplementary table S1 in Finney et al. 2010) was used as an outgroup for both analyses.

Statistical methods

In a given host species, different host-symbiont combinations can differ in their physiology (Goulet et al. 2005). Therefore, we excluded from statistical analyses gorgonian-*Symbiodinium* ITS2 type combinations represented by three or fewer colonies. The sample sizes given in the results reflect the number of colonies used in the statistical analyses. Each parameter was analyzed using a one-way ANOVA with gorgonian species as a factor. Residuals for most parameters were not normally distributed and/or had unequal variance among species. Therefore, most data required transformation. When significant differences were found among gorgonian species, Tukey HSD post hoc tests were used to identify significant differences among all pairwise species combinations. $a^*_{\text{chl } a}$ data could not be transformed to meet the assumptions of ANOVA and was tested by determining the frequency of obtaining an F statistic greater than or equal to the observed F statistic in 10,000 permutations of the data.

Results

Photochemical efficiency of photosystem II in *Symbiodinium*

Measuring the effective ($\Delta F/ F_m'$) and maximum (F_v/F_m) quantum yield of PSII throughout the acclimation period enabled us to calculate maximum excitation pressure over photosystem II, Q_m. Q_m ranged from 0.25 in *P. wagenaari* to 0.32 in *P. anceps* and did not significantly differ between the four species. The Q_m values demonstrated that there was no detrimental tank effect on the gorgonians.

Oxygen flux in gorgonian branches

P-E curves for gorgonian branches did not reach saturation despite being exposed to more than 1800 μmol quanta m^{-2} s^{-1}. Therefore, the maximum photosynthetic rate could not be determined as in Platt et al. (1980). Since 1800 μmol quanta m^{-2} s^{-1} was the highest irradiance shared between the two respirometric chambers, the fitted values at 1800 μmol quanta m^{-2} s^{-1} were used as a proxy for the maximum photosynthetic rates. *P. porosa* and *P. wagenaari* had the highest average photosynthetic rates per cm^2 at 1800 μmol quanta m^{-2} s^{-1} (Figure 1A), with both species having similar gross photosynthetic and respiration rates per cm^2, although *P. porosa* had significantly higher net photosynthetic rates per cm^2 than *P. wagenaari* (Table 1). *P. porosa* also had significantly higher photosynthetic (gross and net) and respiration rates per cm^2 than either *P. anceps* or *E. tourneforti*. On the other hand, *P. wagenaari* exhibited similar photosynthetic (gross and net) and respiration rates per cm^2 to *P. anceps* and similar net photosynthetic rates per cm^2 to *E. tourneforti*. *P. anceps* had significantly higher respiration rates per cm^2 than *E. tourneforti*, but the two species did not differ significantly in their maximum photosynthetic rates per cm^2. When integrated on a diurnal cycle, the total oxygen produced via photosynthesis (10.3 to 25.9 μmol O_2) was less than the oxygen consumed via respiration (13.4 to 29.7 μmol O_2) for each gorgonian species and therefore the 24 h gross P/R were less than 1 (Table 1).

The gross and net photosynthetic rates per *Symbiodinium* cell exhibited a different pattern than the photosynthetic rates per cm^2 (Table 1). *P. anceps* had significantly higher gross and net photosynthetic rates per cell than all other species (Figure 1B, Table 1). *P. porosa* had the second highest average photosynthetic rates per cell, which were significantly higher than those of *P.*

wagenaari, but not *E. tourneforti.* Photosynthetic rates per cell of *E. tourneforti* were similar to both *P. porosa* and *P. wagenaari*.

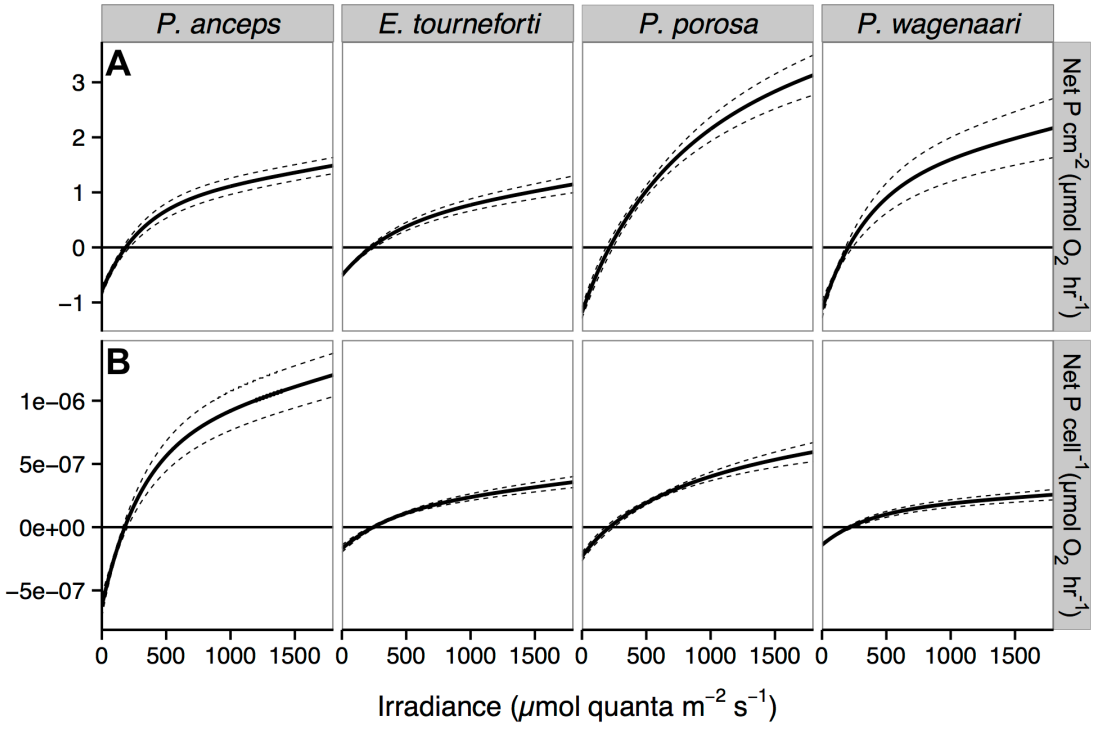

Figure 1. *Symbiodinium* net photosynthesis-irradiance (P-E) curves from four Caribbean gorgonian species.
(A) P-E curves per cm2 of gorgonian branches and, (B) P-E curves per *Symbiodinium* cell. Solid lines represent the average fitted values for *Pterogorgia anceps* (n=9), *Eunicea tourneforti* (n=8), *Pseudoplexaura porosa* (n=6), and *Pseudoplexaura wagenaari* (n=6). Dotted lines represent ± standard error. The photosynthetic rate at 1800 µmol quanta was used as a proxy for the maximum photosynthetic rate.

Table 1. Photosynthesis-irradiance (P-E) curve parameters for gorgonian species.
Sample sizes for each gorgonian species are given in parentheses next to the species name (see Figure 1 legend for full genus names). P and R represent photosynthetic and respiration in μmol O_2 hr^{-1} rates at 1800 μmol quanta m^{-2} s^{-1}, respectively. α represents the initial slope of the P-E curve. Table cells contain the sample mean ± standard deviation. The mean square (MS), F statistics (F), and significance value (p) are from a one-way ANOVA using gorgonian species as a factor. All variables were transformed prior to conducting ANOVA. Means with different superscript letters are statistically different (α=0.05). Power (1- β) is shown for non-significant results.

	Gorgonian species				**One-way ANOVA**			
	***P. anceps* (9)**	***E. tourneforti* (8)**	***P. porosa* (6)**	***P. wagenaari* (6)**	**MS**	**$F_{3, 25}$**	**p**	**1-β**
gross P cm^{-2}	$2.28^{ac} \pm 0.61$	$1.66^{a} \pm 0.48$	$4.32^{b} \pm 1.05$	$3.30^{bc} \pm 1.07$	0.22	10.47	< 0.001	
net P cm^{-2}	$1.49^{a} \pm 0.44$	$1.15^{a} \pm 0.43$	$3.13^{b} \pm 0.89$	$2.17^{a} \pm 0.70$	0.24	8.59	< 0.001	
R cm^{-2}	$-0.79^{a} \pm 0.25$	$-0.51^{b} \pm 0.09$	$-1.19^{c} \pm 0.25$	$-1.12^{ac} \pm 0.38$	0.19	12.12	< 0.001	
gross P μg^{-1} chl *a*	$1.04^{a} \pm 0.39$	$0.71^{a} \pm 0.18$	$0.32^{b} \pm 0.08$	$0.15^{c} \pm 0.03$	0.99	52.60	< 0.001	
net P μg^{-1} chl *a*	$0.68^{a} \pm 0.25$	$0.48^{a} \pm 0.12$	$0.23^{b} \pm 0.05$	$0.10^{c} \pm 0.02$	1.00	46.70	< 0.001	
gross P $cell^{-1} *10^{-7}$	$18.29^{a} \pm 7.35$	$5.27^{bc} \pm 1.95$	$8.28^{b} \pm 2.52$	$3.98^{c} \pm 0.70$	0.50	27.46	< 0.001	
net P $cell^{-1} *10^{-7}$	$12.04^{a} \pm 5.14$	$3.57^{bc} \pm 1.23$	$5.95^{b} \pm 1.84$	$2.57^{c} \pm 0.40$	0.44	22.90	< 0.001	
$\alpha *10^{-3}$ (P μg^{-1} chl *a*)	$2.51^{a} \pm 1.25$	$1.26^{b} \pm 0.57$	$0.53^{c} \pm 0.22$	$0.32^{c} \pm 0.10$	1.11	29.36	< 0.001	
24 h gross P / R	0.88 ± 0.21	0.78 ± 0.23	0.93 ± 0.16	0.83 ± 0.18	0.03	0.78	0.516	0.22

Photosynthetic rates per chlorophyll *a* produced a similar pattern as photosynthetic rates per cell (Table 1). *P. anceps* had the highest average photosynthetic rates per chlorophyll *a* (gross and net), significantly higher than the two *Pseudoplexaura* species, but similar to *E. tourneforti*. The two *Pseudoplexaura* species had significantly lower photosynthetic rates per chlorophyll *a* than *E. tourneforti*, and *P. wagenaari* had significantly lower rates than *P. porosa*. Differences in the initial slope of the P-E curve, α, mirrored differences in photosynthetic rates per chlorophyll *a*, as α was significantly greater for *P. anceps* than all other species (Table 1). α of *E. tourneforti* was significantly greater than in both *Pseudoplexaura* species, which had statistically similar α.

Oxygen flux of isolated *Symbiodinium*

Photosynthetic rates of isolated *Symbiodinium* were lower than the *in hospite* photosynthetic rates except for *Symbiodinium* from *E. tourneforti* (Table 2). With the exception of *Symbiodinium* from *E. tourneforti,* isolated *Symbiodinium* had gross P_{max} / R less than or equal to one (Table 2). The initial slopes of the P-E curves (α) were greater for isolated *Symbiodinium* (Table 2) than for *Symbiodinium* within gorgonian branches (Table 1).

Symbiodinium density

Symbiodinium densities in *P. porosa* were similar to those in *P. wagenaari* and *E. tourneforti*, although *P. wagenaari* had significantly higher densities than *E. tourneforti* (Figure 2A, Table 3). *Symbiodinium* densities in *P. anceps* were significantly lower than in all other species.

Chlorophyll content

P. porosa and *P. wagenaari* had significantly more chlorophyll *a* and c_2 per cm^2 than *P. anceps* and *E. tourneforti* (Table 3). *P. wagenaari* also had significantly more chlorophyll c_2 per cm^2 than *P. porosa* while *P. anceps* and *E. tourneforti* had similar chlorophyll c_2 per cm^2. On the other hand, *P. porosa*, *P. wagenaari*, and *P. anceps* had statistically similar chlorophyll *a* per *Symbiodinium* cell, with *Symbiodinium* in *E. tourneforti* having significantly lower chlorophyll *a* per cell than all other *Symbiodinium* (Figure 2B, Table 3). While chlorophyll c_2 per *Symbiodinium* cell exhibited a similar pattern to chlorophyll *a* per cell, the statistical results were slightly different: *Symbiodinium* in *P. porosa* and *P. wagenaari* had similar chlorophyll c_2 per cell, but only *Symbiodinium* in *P. porosa* had significantly greater chlorophyll c_2 per cell than those in *P. anceps* (Figure 2B, Table 3). *Symbiodinium* in *E. tourneforti* had lower chlorophyll c_2 per cell than *Symbiodinium* in both *Pseudoplexuara* species, but similar chlorophyll c_2 per cell as those in *P. anceps. Symbiodinium* in *P. porosa* and *P. wagenaari* had statistically similar ratio of

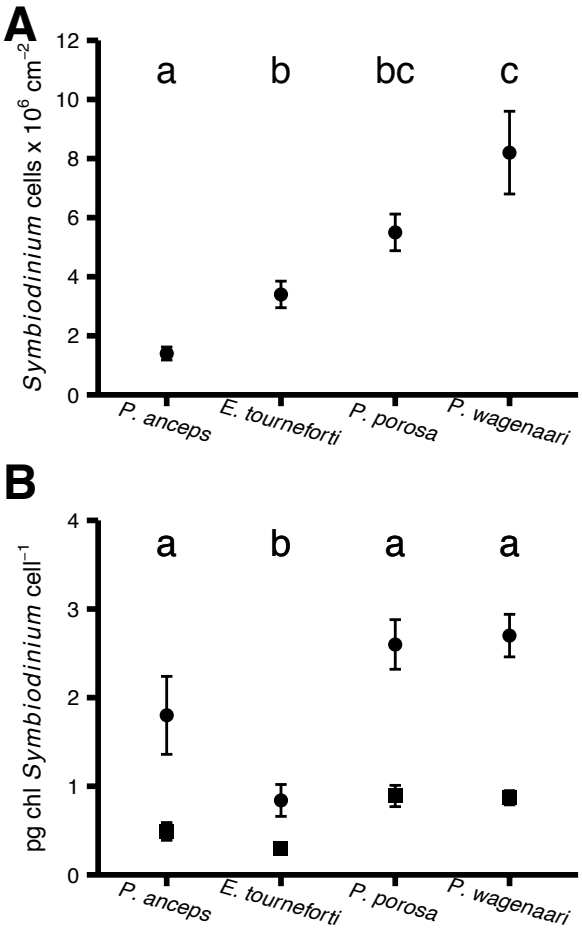

Figure 2. *Symbiodinium* parameters in four Caribbean gorgonian species.
(A) Cell densities and, (B) Concentration of chlorophylls *a* (circles) and c_2 (squares) per *Symbiodinium* cell. Points represent sample means ± standard error. Gorgonian species that do not share a letter are significantly different from each other in either density or chlorophyll *a* per cell (α=0.05, see Figure 1 for full species names and sample sizes). See Table 3 for significant differences in chlorophyll c_2 per cell.

chlorophyll *a* to chlorophyll c_2 to those in *E. tourneforti* and *P. anceps*, but *Symbiodinium* in *E. tourneforti* had a significantly lower ratio of chlorophyll *a* to chlorophyll c_2 than those in *P. anceps* (Table 3).

Chlorophyll *a* specific absorption

P. porosa had the highest estimated absorbance at 675 nm ($D_{c\,675}$), which was significantly greater than that in *P. anceps* and *E. tourneforti*, but similar to *P. wagenaari* (Figure 3A, Table 3). In concordance with chlorophyll density, chlorophyll *a* specific absorption ($a^*_{chl\,a}$), was significantly higher in *E. tourneforti* and *P. anceps* than in the two *Pseudoplexaura* species (Figure 3B, Table 3). *P. wagenaari* had significantly lower $a^*_{chl\,a}$ than all other species.

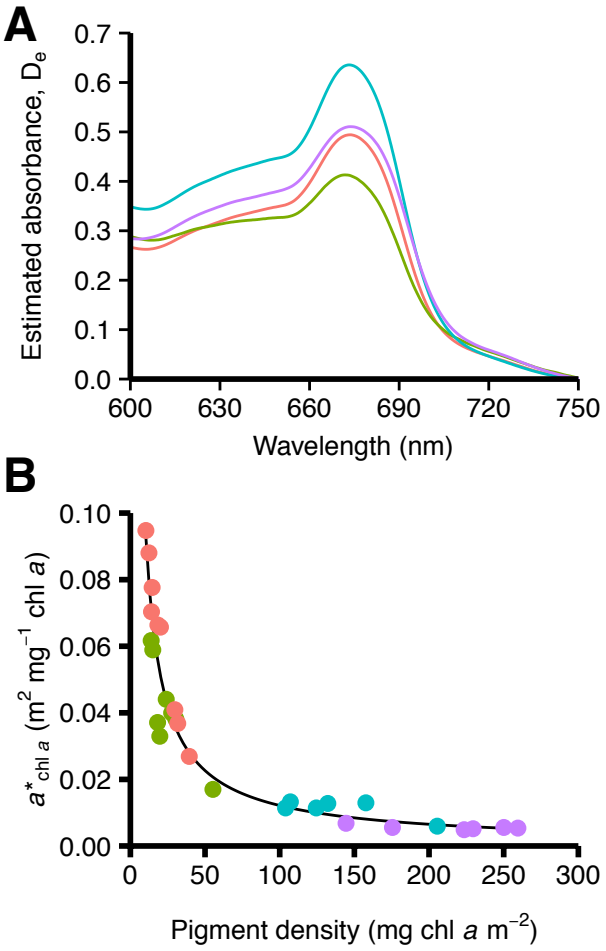

Figure 3. Estimated absorbance, D_e, spectra (A), and chlorophyll *a* specific absorption, $a^*_{chl\,a}$, as a function of pigment density (B), in four Caribbean gorgonian species.
Pterogorgia anceps (red line; n=9), *Eunicea tourneforti* (green line; n=8), *Pseudoplexaura porosa* (blue line; n=6), and *Pseudoplexaura wagenaari* (purple line; n=6). Lines in (A) represent average D_e spectra for each species. The equation for the line in (B) is $y=0.7586*(x^{-0.8976})$.

Table 2. Photosynthesis-irradiance (P-E) curve parameters for isolated *Symbiodinium*.
Sample sizes for isolates from each gorgonian species (see Figure 1 legend for full genus names) are given in parentheses next to the species name. P_{max} and R represent the maximum photosynthetic and respiration rates, respectively, in µmol O_2 hr^{-1}. α is the initial slope of the P-E curve. Table cells contain the sample mean ± standard deviation. The mean square (MS), F statistics (F), and significance value (p) from a one-way ANOVA using gorgonian species as a factor are shown for each variable. All variables were transformed prior to conducting the ANOVA. Means with different superscript letters are statistically different (α=0.05).

	Gorgonian species				One-way ANOVA		
	***P. anceps* (9)**	***E. tourneforti* (8)**	***P. porosa* (6)**	***P. wagenaari* (6)**	**MS**	**$F_{3, 25}$**	**p**
net P_{max} μg^{-1} chl *a*	$-0.01^{a} \pm 0.06$	$0.36^{b} \pm 0.21$	$-0.01^{a} \pm 0.01$	$0.01^{a} \pm 0.02$	0.03	27.47	< 0.001
net P_{max} $cell^{-1} * 10^{7}$	$-0.00^{a} \pm 1.10$	$2.47^{b} \pm 1.47$	$-0.32^{a} \pm 0.18$	$0.08^{a} \pm 0.36$	0.30	7.66	< 0.001
R $cell^{-1} * 10^{7}$	$-2.27^{a} \pm 0.96$	$-1.81^{ac} \pm 0.99$	$-0.62^{b} \pm 0.28$	$-1.06^{bc} \pm 0.48$	0.12	10.01	< 0.001
$\alpha * 10^{-3}$ (P μg^{-1} chl *a*)	$4.23^{ab} \pm 2.37$	$7.57^{a} \pm 4.71$	$2.01^{bc} \pm 1.25$	$1.10^{c} \pm 0.62$	0.45	13.19	< 0.001
gross P_{max} / R	$0.41^{a} \pm 0.18$	$2.65^{b} \pm 0.55$	$0.15^{a} \pm 0.09$	$0.83^{a} \pm 0.46$	0.16	16.30	< 0.001

Table 3. Photosynthetic characteristics of *Symbiodinium* in four Caribbean gorgonian species.
Sample sizes for each gorgonian species (see Figure 1 legend for full genus names) are given in parentheses next to the species name. Parameters include the abundant *Symbiodinium* (*Sym*) internal transcribed spacer region two (*Sym* ITS2) type; *Sym* cell density; chlorophyll content (chl), estimated absorbance at 675 nm ($D_{e\,675}$), chlorophyll *a* specific absorption coefficient of at 675 nm ($a^*_{chl\,a}$), as well as the pressure over photosystem II (Q_m). Table cells contain the sample mean ± standard deviation. The mean square (MS), F statistics (F), and significance value (p) from a one-way ANOVA, using gorgonian species as a factor, are shown for each variable. All variables except $a^*_{chl\,a}$ were transformed prior to conducting the ANOVA. $a^*_{chl\,a}$ could not be transformed to meet the assumptions of ANOVA and was tested using a one-way randomization test and subsequent pair-wise permutations. Means with different superscript letters are statistically different (α=0.05). Power (1- β) is shown for non-significant results.

	Gorgonian species				**One-way ANOVA**			
	***P. anceps* (9)**	***E. tourneforti* (8)**	***P. porosa* (6)**	***P. wagenaari* (6)**	**MS**	**$F_{3,25}$**	**p**	**1-β**
Sym ITS2 type	B1	B1L	B1i	B1				
Sym density (10^6 cells cm^{-2})	$1.43^{a} \pm 0.67$	$3.45^{b} \pm 1.3$	$5.47^{bc} \pm 1.53$	$8.20^{c} \pm 3.43$	0.84	26.62	< 0.001	
chl *a* (pg $cell^{-1}$)	$1.80^{a} \pm 1.32$	$0.84^{b} \pm 0.51$	$2.62^{a} \pm 0.69$	$2.70^{a} \pm 0.60$	0.49	10.40	< 0.001	
chl c_2 (pg $cell^{-1}$)	$0.49^{ab} \pm 0.31$	$0.31^{a} \pm 0.16$	$0.89^{c} \pm 0.30$	$0.87^{bc} \pm 0.19$	0.38	10.90	< 0.001	
chl *a* / chl c_2	$3.56^{a} \pm 0.40$	$2.65^{b} \pm 0.67$	$2.99^{ab} \pm 0.30$	$3.10^{ab} \pm 0.25$	1.19	5.83	0.004	
chl *a* (µg cm^{-2})	$2.13^{a} \pm 1.01$	$2.55^{a} \pm 1.33$	$13.85^{b} \pm 3.81$	$21.38^{b} \pm 4.60$	1.80	75.38	< 0.001	
chl c_2 (µg cm^{-2})	$0.59^{a} \pm 0.26$	$1.00^{a} \pm 0.56$	$4.68^{b} \pm 1.41$	$6.92^{c} \pm 1.53$	63.49	67.60	< 0.001	
$D_{e\,675}$	$0.49^{a} \pm 0.05$	$0.40^{a} \pm 0.08$	$0.65^{b} \pm 0.14$	$0.51^{ab} \pm 0.08$	0.07	9.23	< 0.001	
$a^*_{chl\,a}$	$0.06^{a} \pm 0.02$	$0.04^{a} \pm 0.01$	$0.01^{b} \pm 0.003$	$0.01^{c} \pm 0.001$		26.40	< 0.001	
Q_m	0.32 ± 0.18	0.28 ± 0.06	0.29 ± 0.07	0.25 ± 0.11	0.01	0.41	0.745	0.133

Genetic identification of *Symbiodinium*

All *P. anceps* colonies harbored B1 *Symbiodinium* (accession AF333511; 2001). Eight of the nine *E. tourneforti* colonies sampled harbored type B1L (accession GU907639; Finney et al. 2010), while one colony harbored type B1 (accession AF333511; LaJeunesse 2001). Six *P. porosa* colonies harbored *Symbiodinium* B1i (accession GU907636; Finney et al. 2010). The remaining three *P. porosa* colonies harbored one of two distinct DGGE profiles with dominant ITS2 sequences identical to type B1 (accession AF333511; LaJeunesse 2001). All *P. wagenaari* colonies harbored type B1 *Symbiodinium,* albeit with a distinct DGGE profile from the B1 symbiont in *P. anceps* (discussed in Finney et al. 2010).

Analysis of microsatellite flanking region sequences revealed that *Symbiodinium* B1 from 16 of 19 gorgonian colonies, representing all four gorgonian species, formed a phylogenetic group with high posterior probability (Figure 4). The B1 *Symbiodinium* in this group included *Symbiodinium* from eight of nine *P. anceps* colonies, one colony each of *E. tourneforti* and *P. porosa* and all six *P. wagenaari* colonies. B1 *Symbiodinium* from three gorgonian colonies (from *P. anceps* and *P. porosa*) placed outside this group, but did not cluster with the *Symbiodinium* B1 lineages from scleractinian corals.

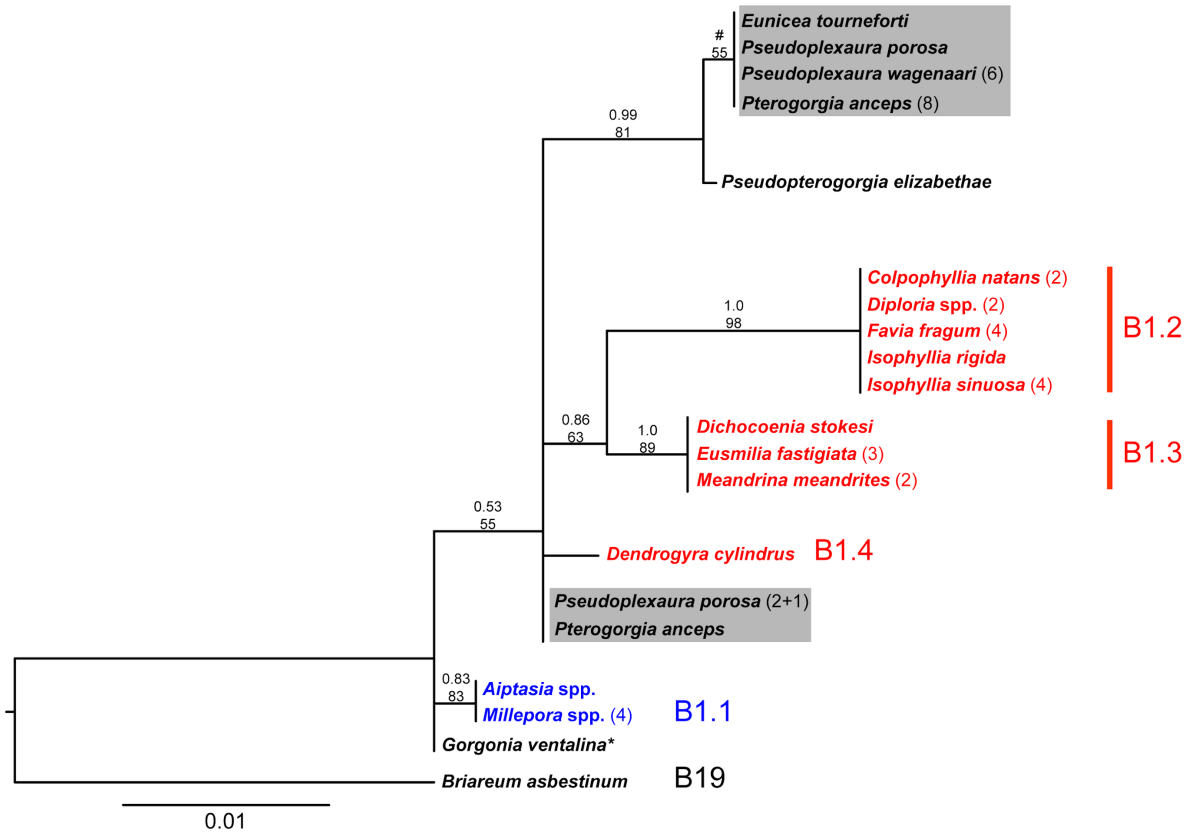

Figure 4. A maximum likelihood phylogenetic tree based on microsatellite flanking regions of B1 *Symbiodinium*.
The phylogeny includes B1 *Symbiodinium* from the four gorgonian species in this study (highlighted in gray), from other gorgonian corals (Thornhill et al. 2013), from scleractinian and hydrozoan corals (Finney et al. 2010), as well as *Symbiodinium minutum* from *Aiptasia*, a sea anemone (Thornhill et al. 2013). Branch tips are labeled with host species and sample sizes when n>1. Gorgonian coral species are shown in black, scleractinian coral species are shown in red, and the other cnidarians are shown in blue. B1 lineages described by Finney et al. (2010) are listed besides the host taxa. Numbers above the branches are the posterior probability above the maximum likelihood consensus support for each group. B1 *Symbiodinium* from 16 of 19 gorgonian colonies sampled clustered in a phylogenetic group with high posterior probability (top gray box). Three gorgonian colonies were placed outside of this clade (bottom gray box) and were most closely related to *Symbiodinium* isolated from *Pseudoplexaura porosa* from Florida (indicated with (+1)) and cultured *Symbiodinium* from *Gorgonia ventalina* (indicated with *, Thornhill et al. 2013). (#) indicates a group with maximum likelihood, but not Bayesian posterior probability support.

Discussion

Gorgonian corals blanket the landscape of Caribbean coral reefs (Cary 1918; Bayer 1961; Ruzicka et al. 2013), yet few data exist on the physiology of their mutualism with *Symbiodinium* (Burkholder and Burkholder 1960; Kanwisher and Wainwright 1967; Lewis and Post 1982; Drohan et al. 2005; Mydlarz and Jacobs 2006; Baker et al. 2011). Unlike scleractinian corals, whose abundance has dramatically declined in the Caribbean (Hughes 1994; Gardner et al. 2003; Pandolfi et al. 2005; Edmunds and Elahi 2007; Ruzicka et al. 2013), gorgonians have withstood recent environmental perturbations. Learning about gorgonian symbioses, at current ambient conditions, enhances our understanding and our ability to predict the future of Caribbean coral reefs. We therefore employed multiple tools to characterize aspects of *Symbiodinium* photosynthesis in four common Caribbean gorgonian species.

Oxygen flux data demonstrated differences in the *Symbiodinium* in the four studied gorgonians. For example, the two *Pseudoplexaura* species had the highest average photosynthetic rates per cm^2, probably due to the higher *Symbiodinium* and chlorophyll densities compared to *P. anceps* and *E. tourneforti*. On the other hand, the two *Pseudoplexaura* species had lower initial slopes of the P-E curves, low photosynthetic rates per *Symbiodinium* cell and per chlorophyll *a,* and lower chlorophyll *a* specific absorption. Taken together, these data suggest that *Symbiodinium* in *P. porosa* and *P. wagenaari* are less efficient in light absorption and utilization than *Symbiodinium* in *P. anceps* and *E. tourneforti.* The light levels available for *Symbiodinium* could differ due to *Symbiodinium* self-shading or to host tissue characteristics such as tissue thickness (Ramus et al. 1976; Kaniewska et al. 2011) or pigmentation.

Looking at changes in chlorophyll a specific absorption coefficient as a function of chlorophyll *a* density further illustrated the differences in photosynthesis between the

Symbiodinium in the four gorgonian species. The $a^*_{\text{chl } a}$ of *Symbiodinium* in *P. anceps* demonstrate a very high pigment light absorption efficiency, comparable to that of *Symbiodinium* in the scleractinian coral *Porites banneri* (Enríquez et al. 2005). *E. tourneforti* $a^*_{\text{chl } a}$ also fell within those previously reported for scleractinian corals. On the other hand, as a function of chlorophyll *a* density, the $a^*_{\text{chl } a}$ values in the two *Pseudoplexaura* species was very low, comparable to those values reported for phytoplankton and freshly isolated *Symbiodinium* (Bricaud et al. 1995; Enríquez et al. 2005).

Of the four gorgonian species, *Symbiodinium* in *P. anceps* exhibited twice the photosynthetic rate per *Symbiodinium* cell than the rate in *Symbiodinium* in the next gorgonian species (*P. porosa*) and the highest average photosynthetic rates per chlorophyll *a*. The relatively high photosynthesis per *Symbiodinium* in *P. anceps* may be related to the low density of *Symbiodinium* and chlorophyll *a* per cm^2. In addition, the thin, angular branches and low polyp density may aid *Symbiodinium* photosynthesis in *P. anceps* by maximizing gas exchange and/or reducing self-shading of *Symbiodinium*.

The four Caribbean gorgonian species produced comparable photosynthetic and respiration rates per cm^2 to the average rates of eight shallow scleractinian coral species (P=2.0, R=0.64; Edmunds et al. 2011). Conversely, the Mediterranean gorgonian *Eunicella singularis* at 15 m depth had lower average *Symbiodinium* photosynthetic (~1) and respiration (~0.55) rates per cm^2 (Ezzat et al. 2013). The differences could be due to *E. singularis* in deeper waters or being exposed to lower irradiance levels than those in the current study (Ferrier-Pages et al. 2009; Ezzat et al. 2013). In our study, the four gorgonian species did not exhibit photoinhibition, similar to what has been observed in other symbioses between *Symbiodinium* and cnidarians (discussed in Fitt and Cook 2001). The lack of photoinhibition may be due to branch tissue

thickness, as was seen in the octocoral *Capnella gaboensis* (Ramus et al. 1976; Farrant et al. 1987). The gross P / R ratios in the four gorgonian symbioses, ranging from 2 to 4, were comparable to ratios for other octocorals (Mergner and Svoboda 1977; Fabricius and Klumpp 1995; Tunn et al. 1996; Khalesi et al. 2011), anemones (Goulet et al. 2005), and shallow water scleractinian corals (Edmunds et al. 2011). On the other hand, the ratios of diurnal integrated gross photosynthesis to respiration were below 1. It remains to be determined the extent of the contribution of the *Symbiodinium* autotrophic production to the energy budget of these Caribbean gorgonians.

Within a host, *Symbiodinium* photosynthesis may be affected by host characteristics (Kaniewska et al. 2008; Kaniewska et al. 2011). For example, the scleractinian coral skeleton enhances light absorption by *Symbiodinium* (Kühl et al. 1995; Enríquez et al. 2005), and *Symbiodinium* chlorophyll *a* specific absorption is higher in symbiosis than in isolation (Enríquez et al. 2005). Chlorophyll *a* specific absorption of *Symbiodinium* in the studied gorgonian corals was comparable to that of scleractinians (Enríquez et al. 2005; Kaniewska et al. 2011), even though gorgonian skeletal structure (sclerites and an axial rod) substantially differs from the calyx structure in scleractinian corals. The calcite sclerites within gorgonian tissues may produce the same effect as the light scattering of the scleractinian coral skeleton, perhaps similar to the influence of the siliceous spicules of sponges on light transmission (Aizenberg et al. 2004; Brümmer et al. 2008).

In symbioses between cnidarians and *Symbiodinium,* photosynthesis depends on the genetic identities of both the host and symbiont (Goulet et al. 2005). Therefore, it is imperative to identify the *Symbiodinium.* In the Caribbean, scleractinian corals host *Symbiodinium* belonging to clades A, B, C, or D (LaJeunesse 2002; Finney et al. 2010). On the other hand, the

majority of Caribbean gorgonian species host only clade B *Symbiodinium* (Goulet and Coffroth 2004; Goulet et al. 2008). The four gorgonian species in this study were no exception, harboring clade B *Symbiodinium* belonging to types B1, B1i, and B1L. Types B1i and B1L have only been reported in Caribbean gorgonian species (Santos et al. 2001; Finney et al. 2010). Sequencing of the B1 *Symbiodinium* from the four gorgonian species revealed that they harbor B1 *Symbiodinium* with distinct microsatellite flanking region sequences from those in scleractinians and that the B1 *Symbiodinium* from most gorgonian colonies formed a distinct group amongst the previously identified B1 lineages from scleractinian corals.

Although both *P. anceps* and *P. wagenaari* hosted type B1 *Symbiodinium,* the photosynthetic characteristics differed between these two symbioses. Photosynthetic variability within *Symbiodinium* type B1 has also been observed in cultures (Hennige et al. 2009), and may be associated with distinct genetic lineages within type B1 (Santos et al. 2004; Finney et al. 2010). In our study, eight of the nine *P. anceps* colonies, and all *P. wagenaari* colonies, harbored symbionts from the same, highly supported, phylogenetic group within B1 *Symbiodinium*. Therefore, the observed photosynthetic variability was not due to different B1 lineages but probably due to the physiology of different host-symbiont combinations (e.g., Goulet et al. 2005).

In *E. tourneforti, Symbiodinium* had comparable photosynthetic rates per cell in the intact symbiosis and in isolation. On the other hand, maximum photosynthetic rates per cell in *Symbiodinium* isolated from *P. anceps, P. porosa*, and *P. wagenaari* were lower than those measured *in hospite,* although the average α was higher in isolation. Diminished photosynthetic rates in isolated *Symbiodinium* cells may occur in the absence of host carbon concentrating mechanisms (Goiran et al. 1996) or differences in carbonic anhydrase activity among

Symbiodinium types (e.g., Brading et al. 2013). Exposure to the ionic environment of seawater (Goiran et al. 1997; Seibt and Schlichter 2001) or bacteria (Wang et al. 2011) may also reduce photosynthesis in isolated *Symbiodinium*. In the sea anemone *Aiptasia pallida*, at ambient temperatures, the photosynthetic rates of isolated *Symbiodinium* were also lower compared to the intact association, although not to the degree measured here (Goulet et al. 2005). Conversely, secondary metabolites released from homogenized gorgonian corals may impair isolated *Symbiodinium*, as reported for homogenate of the soft coral *C. gaboensis* that lysed *Symbiodinium* cells (Sutton and Hoegh-Guldberg 1990). Therefore, secondary metabolites produced by many gorgonians may limit the utility of investigating freshly isolated *Symbiodinium.*

In conclusion, my results contribute to critical data on *Symbiodinium* physiological performance in their mutualism with four Caribbean gorgonian species at ambient temperature. Given that gorgonian corals are either maintaining or increasing their abundance on Caribbean coral reefs, understanding aspects of their symbiosis is imperative to understanding the future of Caribbean coral reefs. This study demonstrates differences between *Symbiodinium* photosynthetic characteristics in the four gorgonian species, collected from the same site, maintained under identical conditions, and with two of the gorgonian species containing the same *Symbiodinium* type. The differences observed between the gorgonian symbioses emphasize the influence of the host physiology and architecture on *Symbiodinium* photosynthesis.

II. *SYMBIODINIUM* PHOTOSYNTHESIS AND THERMAL TOLERANCE OF THE TWO MORPHOLOGIES OF *BRIAREUM ASBESTINUM*

Introduction

The morphology of sedentary organisms such as corals (scleractinian and octocorals) is influenced by the organism's genetic makeup, environmental conditions, and ecological interactions (reviewed in Todd 2008). Corals grow in a variety of morphologies, contributing to the structural diversity of the coral reef habitat (Odum and Odum 1955). Scleractinian coral species exhibit massive, encrusting, plating, or branching colony morphologies (Veron and Stafford-Smith 2000). In octocoral species, colonies grow in branching, rod, fan or encrusting morphologies, and the morphology is often used as one of the characters to distinguish between different coral species (Bayer 1961).

Coral colony morphology, in both scleractinian corals and octocorals is sometimes flexible. Under different environmental conditions, for example, across environmental gradients of water flow (Sebens 1984; Chang et al. 2007) depth (West et al. 1993; Prada et al. 2008), sedimentation, irradiance, water temperature or salinity (Bruno and Edmunds 1997) colonies of the same coral species can exhibit morphological differences. These differences can be in whole colony characteristics, such as branch numbers, branch widths, branch geometry (Gutierrez-Rodriguez et al. 2009) or colony height (West et al. 1993; Kim et al. 2004; Prada et al. 2008) and/or changes in skeletal characteristics, such as corallite architecture and density

in scleractinian corals (Bruno and Edmunds 1997) or sclerite density in octocorals (Kim et al. 2004; Gutierrez-Rodriguez et al. 2009). For example, in the octocoral *Briareum asbestinum* (Pallas 1766), branching colonies can vary in height, branch width, and sclerite characteristics across depths (West et al. 1993).

Some of the morphological changes in corals over depth can be associated with the fact that scleractinian corals and many octocorals host endosymbiotic dinoflagellate algae belonging to the genus *Symbiodinium*. These symbionts transfer part of their photosynthate to their host (Muscatine and Cernichiari 1969; Muscatine et al. 1984). Changes in coral morphology over depth coincide with a reduction in irradiance, and some changes in host morphology at depth, such as thinner branches or flatter surfaces (Todd 2008), may augment *Symbiodinium* photosynthesis (Hoogenboom et al. 2008). Within species coral morphological variation can be explained by different environmental conditions, but those conditions may contribute to intraspecific genetic divergence (Todd 2008). Depth divides populations of the octocorals *B. asbestinum* (Brazeau and Harvell 1994) and *Eunicea flexuosa* (previously *Plexaura flexuosa* sensu Grajales et al. 2007; Prada and Hellberg 2013).

As opposed to morphological changes over environmental gradients, some coral species exhibit different morphologies in the same habitat. For example, the scleractinian coral *Porites* occurs in both a branching and mounding morphospecies (Forsman et al. 2009), and the scleractinian coral *Montipora capitata* has a both a plating and a branching morphology at the same depth (Padilla-Gamiño et al. 2012). The octocoral *B. asbestinum* exhibits a branching morphology in shallow and deep habitats (Goldberg 1973; Dahlgren 1989) but also an encrusting morphology that has only been observed in shallow waters (originally *Ammothea polyanthes*

sensu Duchassaing and Michelotti 1860). Since the two morphologies of *B*. *asbestinum* co-occur on shallow patch reefs (Cairns 1977; Brazeau and Harvell 1994), *B*. *asbestinum* provides a study system that uncouples the effect of the environment on host morphology.

In *B*. *asbestinum* one can focus on *Symbiodinium* photosynthesis in two host morphologies under the same environmental conditions. One can also evaluate how the *Symbiodinium* in the two distinct morphologies respond to potential stressors. For example, increases in sea surface temperature can detrimentally affect *Symbiodinium* photosynthesis (Warner et al. 1999) and lead to a reduction in *Symbiodinium* density and chlorophyll concentrations, known as coral bleaching (Brown 1997). Bleaching is considered a stress response and can lead to the death of the host colony (reviewed in Weis 2008). Coral species with different morphologies can respond differently to stressors (Loya et al. 2001; van Woesik et al. 2011). How do colonies of the same species, but with different morphologies cope with environmental change? The objectives of this study was to investigate *Symbiodinium* photosynthesis in the two different *B. asbestinum* morphologies both at ambient and elevated temperature.

Methods

Sample collection

In June 2012, eight encrusting and eight branching colonies of *Briareum asbestinum* were sampled at 5 m depth from the reef La Bocana Chica (20° 52' N, 86° 50' W) near Puerto Morelos, Quintana Roo, México. Four pieces were collected from each colony, either as fragments from the encrusting colonies or branches from the branching colonies. One piece from each colony was immediately frozen at -80 °C. This piece provided information on colonies in

the field and whether the ambient conditions in the experiment reflected field conditions. The other three pieces from each of the encrusting or branching colonies were placed in experimental aquaria in a flowing seawater system at the Unidad Académica Puerto Morelos, Instituto de Ciencias del Mar y Limnología, Universidad Nacional Autónoma de México. In order to maintain their natural orientation, fragments of encrusting colonies were attached to horizontal acrylic tiles, and branches from the branching colonies were attached to vertical PVC stands. Using meshes, solar irradiance reaching the aquaria was reduced by 60%, to attain irradiance levels similar to those at the collection depth.

Experimental conditions and photochemical efficiencies

For 11 days following collection, temperature in the experimental aquaria was maintained at 29.5 °C (± 0.4 SD), similar to the ambient seawater temperature during the summer months (May-August) on shallow reefs in the area (Rodríguez-Martínez et al. 2010). The photochemical efficiency of photosystem II was measured daily, at solar noon ($\Delta F/F_m'$; effective yield) and after dusk (F_v/F_m; maximum yield), using a pulse amplitude modulated (PAM) fluorometer (Walz, Effeltrich, Germany). The end of the PAM fiber optic cable was fitted with clear polypropylene tubing to maintain a constant distance between the cable and the surface of *B. asbestinum*. After 11 days in the aquaria, the photochemical efficiency of *Symbiodinium* remained constant, ending the acclimation period. At this point, the second piece from each colony was sampled, either 11 or 12 days post collection, and served as a control for the aquarium conditions.

Following acclimation, the third piece from each colony remained in the ambient 29.5 °C seawater aquarium, while the fourth piece from each colony was moved to an aquarium in which the seawater temperature was increased 1°C per day up to 32.0 °C (± 0.4 SD), which represents a

3 °C increase above typical summer temperatures and represents a predicted average sea surface temperature by 2099 (IPCC, 2007). Once the elevated temperature aquarium reached 32.0 °C, the respective pieces were maintained in the ambient and elevated temperature treatments for approximately 7 days. Due to the length of time required to measure oxygen flux, the sampling of *B. asbestinum* pieces held in the aquaria at 29.5 °C and 32.0 °C, respectively, was staggered: *B. asbestinum* from the aquarium maintained at 32.0 °C were sampled after 7 or 8 days of exposure to 32.0 °C, while *B. asbestinum* from the aquarium held at 29.5 °C since collection were sampled after 6 or 9 days from the start of the experiment.

Throughout the experiment, the photochemical efficiency of photosystem II of *Symbiodinium* in both *B. asbestinum* morphologies was measured daily, at solar noon ($\Delta F/F_m'$; effective yield) and after dusk (F_v/F_m; maximum yield). Using the effective and maximum yield values obtained, we calculated the maximum excitation pressure over photosystem II, Q_m, for each morphology, whereby $Q_m = 1-((\Delta F/F_m') / (F_v/F_m))$ (Iglesias-Prieto et al. 2004). Both downwelling and horizontal irradiance (400-700 nm) were measured at solar noon throughout the experiment using a cosine corrected sensor.

Oxygen flux

On the day of sampling, the fragment or branch were placed into a 0.5 l acrylic chamber. Oxygen flux was measured simultaneously in two such chambers. Within the chambers, 0.45 µm filtered seawater was circulated using a small pump, while a temperature-controlled water jacket maintained constant temperature. A 782 Oxygen Meter (Strathkelvin Instruments Ltd., North Lanarkshire, Scotland) recorded the oxygen flux measured by Clark-type oxygen electrodes, which were calibrated at either 29.5 or 32.0 °C by bubbling oxygen and nitrogen gas. *B.*

asbestinum was sealed in the chambers for 30 minutes in the dark. During the final 10 minutes of darkness, oxygen flux was recorded to calculate the respiration rate (R).

B. asbestinum was then illuminated on one side using three 6W LED bulbs, with the white sides of the chambers reflecting the light within each chamber. Between the light source and the chamber where layers of window screening.. *B. asbestinum* was exposed to 12, increasing, irradiance levels (0-3000 μmol quanta m^{-2} s^{-1}) by removing layers of window screening between the LED bulbs and the chambers. Each irradiance level was measured using a Walz 4π quantum sensor (Effeltrich, Germany) and lasted until a linear change in oxygen concentration was recorded. After the final irradiance level, the chambers were darkened and post-illumination respiration was measured for 10 min.

Gross photosynthetic rates were plotted against irradiance to generate *B. asbestinum* photosynthesis-irradiance curves, which were modeled using the equation of Platt et al. (1980). Since *B. asbestinum* photosynthetic rates did not reach saturation, the maximum photosynthetic rate could not be calculated as described by Platt et al. (1980). Therefore, the maximum photosynthetic rate of each piece was approximated from the fitted photosynthetic rate at 2800 μmol quanta m^{-2} s^{-1} (P), which was the greatest common irradiance level in both chambers. The initial slope of the P-E curves, α, was compared after standardization to chl^{-1} *a*. The saturation irradiance, E_k, was calculated as P/α. The compensation irradiance for each sample, E_c, was determined as the lowest fitted irradiance value with a positive net photosynthetic rate.

Rates of oxygen flux were standardized to *B. asbestinum* surface area, which was measured using the aluminum foil method (Marsh 1970), the number of *Symbiodinium* cells, chlorophyll *a* content, and the amount of protein in the *B. asbestinum* piece. From each fragment

or branch, a subsection was sampled for subsequent *Symbiodinium* isolation and its surface area was also determined using the aluminum foil method (Marsh 1970). The subsection and the rest of the tissue were frozen at -80 °C.

Symbiodinium density and chlorophyll concentrations

Symbiodinium cells were isolated from the frozen *B. asbestinum* subsection by homogenizing the subsection in a mortar and pestle. The homogenate volume was brought up to 20 ml with 0.45 µm filtered seawater and centrifuged for 1 min at 500 rpm to remove sclerites. The liquid fraction, which contained the *Symbiodinium*, was filtered through 150, 74, and 20 µm nitex meshes, centrifuged (1 min at 3500 rpm), and washed two more times with 10 ml of filtered seawater. *Symbiodinium* cells were resuspended in 5 ml of filtered seawater and aliquoted for measurement of cell density (1 ml), chlorophyll concentration (1 ml), and *Symbiodinium* genetic identification (2 ml).

The number of *Symbiodinium* cells was determined using four replicate hemocytometer counts (4 mm^2 each) of the 1 ml aliquot. The total number of *Symbiodinium* cells in the solution was standardized to the surface area of the homogenized subsection (cells cm^{-2}). For oxygen flux measurements, the total number of *Symbiodinium* cells in the *B. asbestinum* piece was calculated using the ratio of the surface area of the entire piece to the surface area of the subsection used for *Symbiodinium* isolation. For each sample taken at collection, *Symbiodinium* estimated spherical diameters were measured for three subaliquots using a FlowCAM Imaging Particle Analyzer (Fluid Imaging Technologies, Maine, USA). *Symbiodinium* were distinguished from other particles based on their diameter and circle fit.

Chlorophylls of isolated *Symbiodinium* were extracted from the respective aliquot using

950 µl of cold 100% acetone and 50 µL DMSO. The absorbance of extracted pigments was measured at 630, 660, and 750 nm using a spectrophotometer (Ocean Optics, Dunedin, Florida, USA). Absorbance at 750 nm was subtracted from the absorbance at 630 nm and 660 nm to account for scattering, the absorbance values were used to calculate chlorophylls *a* & c_2 concentrations following (Jeffrey and Humphrey 1975), and the concentrations were standardized to *Symbiodinium* density (pg chl cell^{-1}) and the surface area of the *B. asbestinum* subsection (µg chl cm^{-2}). For oxygen flux measurements, the amount of chlorophyll *a* in the *B. asbestinum* piece used in the respirometry chamber was calculated using the ratio of the surface area of the entire piece to the surface area of the subsection used for *Symbiodinium* isolation.

Light absorption

Estimated absorbance (D_e) of *B. asbestinum* tissue was measured every alternate evening throughout the duration of the experiment. *B. asbestinum* were illuminated from all sides and spectral reflectance was measured using a fiber optic spectrophotometer (Ocean Optics, Dunedin, Florida, USA). Spectral reflectance was standardized to the reflectance of a dried *B. asbestinum* fragment or branch, which was painted white, to control for light scattered by the octocoral surface. Reflectance spectra were converted to D_e spectra using a negative log function and D_{e750} was subtracted from $D_{e400\text{-}750}$ to account for residual scattering. The specific absorption coefficient of chlorophyll *a* ($a^*_{\text{chl } a}$) was calculated as $a^*_{\text{chl } a} = (D_{e675} / \rho) \times \ln(10)$, where ρ is mg m^{-2} of chlorophyll *a* (Rodríguez-Román et al. 2006).

Symbiodinium type and cell size

Symbiodinium was identified using the internal transcribed spacer 2 region (ITS2) of

ribosomal DNA (LaJeunesse and Trench 2000). DNA of isolated *Symbiodinium* was extracted from all fragments and branches using a modified CTAB protocol (Goulet and Coffroth 2004). The ITS2 region was amplified using the primers ITSintfor2, ITS-Reverse, and ITS2CLAMP (LaJeunesse and Trench 2000). ITS2 amplicons were visualized using denaturing gradient gel electrophoresis (45-80% denaturant run at 100 V for 16 h; LaJeunesse 2002). Dominant ITS2 sequence variants were excised from the electrophoresis gel, reamplified using ITSintfor2 and ITS-Reverse, cleaned using ExoSAP-IT (Affymetrix, CA, USA), and sequenced at the DNA Laboratory at Arizona State University. DNA sequences were compared to the *Symbiodinium* sequences in GenBank to identify the *Symbiodinium* type.

Briareum asbestinum genetics

For *B. asbestinum* host identification, DNA was extracted from seven frozen fragments and six branches using a modified CTAB protocol (Goulet and Coffroth 2004). The DNA mismatch repair gene, *msh1,* was amplified from each colony using the primers ND42599F and Mut3458R (Sánchez et al. 2003). Amplicons were cleaned using ExoSAP-IT (Affymetrix, CA, USA), and sequenced at the DNA Laboratory at Arizona State University. Sequences were aligned with the available *Briareum msh1* sequences in GenBank.

Briareum asbestinum protein content

To compare the biomass of encrusting and branching *B. asbestinum,* protein content was measured. Protein was extracted from the *B. asbestinum* pieces maintained for seven days in the ambient or the elevated aquaria. Samples were freeze-dried for 24 h and then incubated in 1 M NaOH for 24 h. Protein content of the sample was determined using the Bio-Rad Protein Assay

(Bio-Rad, USA). Triplicate absorbance measurements were taken on each sample and the average absorbance was compared to the absorbance of bovine serum albumin standards. The amount of protein extracted was standardized to the surface area of the freeze-dried *B. asbestinum*. The total amount of protein in the entire *B. asbestinum* piece was calculated using the ratio of the surface area of the subsection used for protein determination to the surface area of the entire piece.

Briareum asbestinum polyp behavior

Throughout the experiment, polyp expansion was recorded daily at solar noon. Polyp expansion was evaluated by eye. Each *B. asbestinum* fragment or branch was categorized according to polyp behavior as either having 0-49% polyps out ("contracted") or 50-100% polyps out ("expanded").

Statistical analyses

In order to limit the variation due to different host genotypes, we placed pieces from the same *B. asbestinum* colonies in both the ambient and elevated temperature aquaria. The data collected at the end of the temperature treatments were analyzed using a linear mixed model fit by restricted maximum likelihood with the following factors: morphology (two levels, fixed), temperature (two levels, fixed), morphology*temperature, and a blocking factor for host colony (16 levels, random). Variables were transformed as needed to satisfy the assumptions of linear models. A second, similar, model was used to compare the photosynthetic characteristics of *B. asbestinum* sampled under ambient temperatures following collection, acclimation, and at the end of the experiment.

Several parameters were analyzed using other statistical tests. A paired t-test was used to

analyze the difference between horizontal and downwelling irradiance over the course of the experiment. *Symbiodinium* diameter was compared between morphologies using a t-test. *B. asbestinum* polyp behavior was analyzed using a chi-square test for independence between polyp expansion (contracted or expanded) and *B. asbestinum* morphology.

Results

Symbiodinium type and cell size

The two morphologies of *Briareum asbestinum* hosted different *Symbiodinium* types. All encrusting *B. asbestinum* fragments harbored *Symbiodinium* with an ITS2 sequence identical to that of type B19 (Accession GU907641; Finney et al. 2010). On the other hand, all *B. asbestinum* branches contained *Symbiodinium* B21 (Accession GU907651; =B38 sensu Finney et al. 2010). The abundant *Symbiodinium* type within each *B. asbestinum* morphology did not change over the course of the experiment and was the same in the field as in the experimental aquaria. The *Symbiodinium* differed in estimated spherical diameter, with B19 (10.2 μm ± 0.3 SD) being significantly larger than B21 (9.7 μm ± 0.4 SD; $t(11)=2.7$, $P=0.019$, $r=0.40$).

Briareum asbestinum genetics

The samples from the encrusting and branching *B. asbestinum* morphologies in our study had identical *msh1* sequences. The sequences from our study were identical to a sequence from both *B. asbestinum* morphologies (Accession FJ434352; Bilewitch et al. 2010), and 2 nucleotides different from another sequence from encrusting *B. asbestinum* (Accession AY533653; Sánchez and Cairns 2004).

Experimental conditions

Based on the parameters measured, the experimental aquaria conditions for the ambient temperature closely reflected the ambient field conditions. The values for *Symbiodinium* density, both chlorophylls cm^{-2}, and both chlorophylls $cell^{-1}$, were not significantly different between field and ambient aquarium conditions for both morphologies (data not shown). The only photosynthetic characteristic that differed significantly between *B. asbestinum* collected in the field and *B. asbestinum* at the end of the experiment at ambient temperature was the ratio of chlorophyll a/c_2, which was 35% greater in encrusting fragments than in branches in the field (encrusting: median=3.1, n=8; branching: median= 2.33, n=8; U=0, $p<0.001$), but was not significantly different between the two morphologies in the aquaria at ambient temperature (encrusting: median=3.6, n=8; branching: median= 3.31, n=7; U=21, p=0.463).

We maintained the fragments and branches in a similar orientation as they would be found in the field. Due to their horizontal orientation, encrusting fragments received significantly more irradiance than branches over the course of the experiment ($t(14)=8.0$, $P<0.001$). Encrusting fragments were exposed at noon to 581 ± 230 (SD) µmol quanta m^{-2} s^{-1} compared to the 200 ± 71 (SD) µmol quanta m^{-2} s^{-1} irradiance exposure for *B. asbestinum* branches. In addition, encrusting fragments experienced larger fluctuations in irradiance, as evidenced by the standard deviation of incident irradiance being three fold greater for encrusting fragments than for branches.

Symbiodinium photochemical efficiency

At ambient temperature, the photochemical efficiency at dusk (F_v/F_m) was not significantly different between the two *B. asbestinum* morphologies at the end of the experiment

(Figure 5a, Table 4, Table 5; t(27)=-2.0, P=0.178, r=0.14). Compared to ambient temperature, elevated temperature significantly reduced F_v/F_m of encrusting fragments by 36% (t(27)=10.2, P<0.001, r=0.81) which was more than double the 14% reduction seen in branches at elevated temperature (t(27)=4.7, P<0.001, r=0.47). Consequently, at elevated temperature, F_v/F_m of encrusting fragments was significantly lower (30%) than that of *B. asbestinum* branches (t(27)=-7.6, P<0.001, r=0.70).

The photochemical efficiency at solar noon ($\Delta F/F_m'$) of encrusting fragments was significantly lower than that of branches at both temperatures, 38% and 34% lower at ambient and elevated temperatures, respectively (Figure 5b, Table 4, Table 5). Elevated temperature caused a similar effect on the $\Delta F/F_m'$ of both morphologies (Table 1), significantly reducing $\Delta F/F_m'$ of encrusting fragments by 20% and branches by 25% compared to $\Delta F/F_m'$ at ambient temperature. The acclimation of both encrusting and branching pieces of *B. asbestinum* to elevated temperatures, as seen by the reduction in effective ($\Delta F/ F_m'$) and maximum (F_v/F_m) yield of PSII, led to no changes in Q_m (Figure 5c).

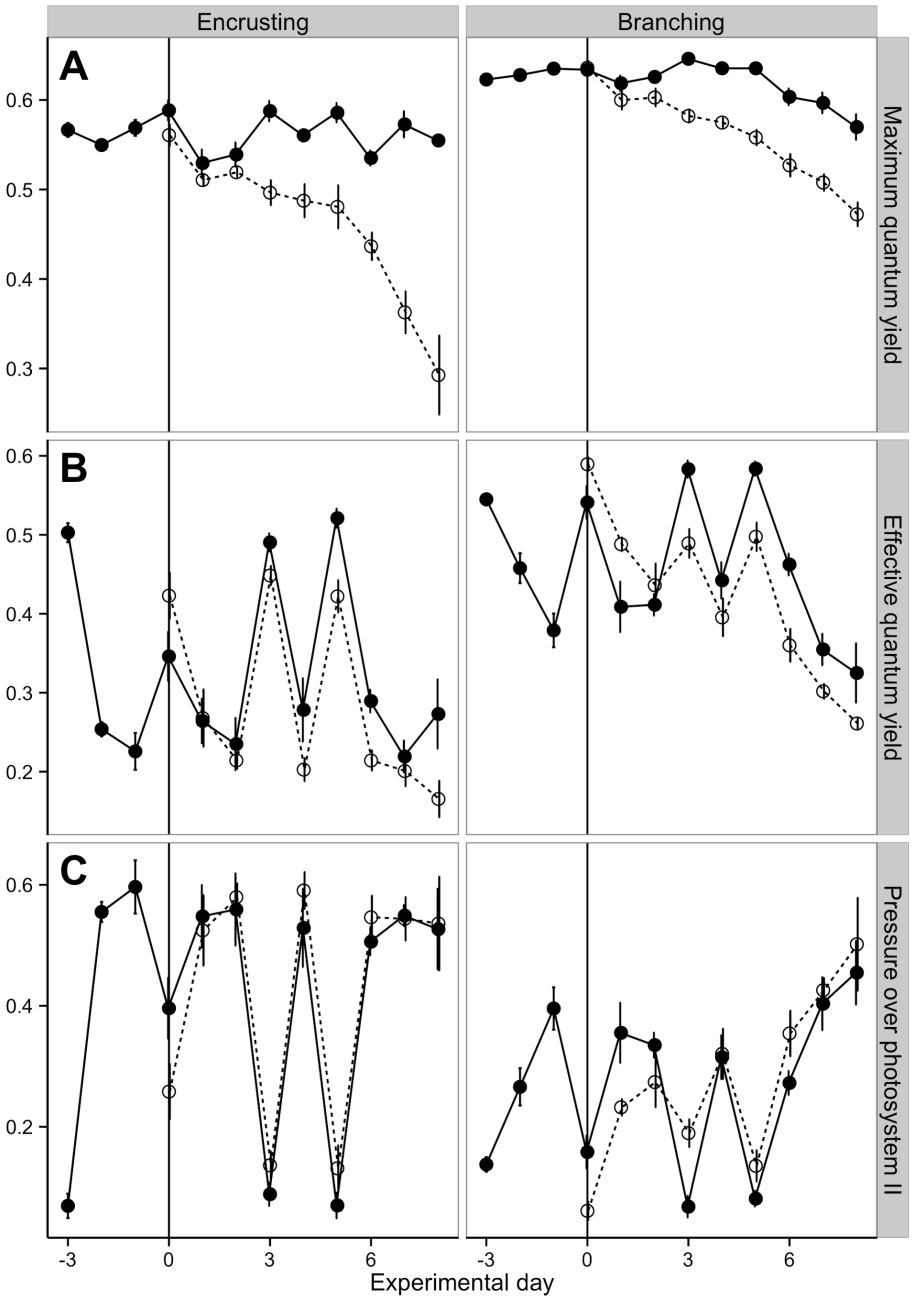

Figure 5. *Symbiodinium* photochemical efficiencies in *Briareum asbestinum* at ambient and elevated temperatures and the pressure over photosystem II during the study.

Symbiodinium photochemical efficiency after dusk (F_v/F_m; maximum yield) (A) and at solar noon ($\Delta F_v/F_m$'; effective yield) (B) at 29.5 °C (solid lines and circles) and at 32.0 °C (dashed lines and open circles). Points and error bars represent means and standard error of the mean, respectively. (C) Pressure over photosystem II (Q_m) At the end of the experiment, n=8 for all treatments except for encrusting fragments at 32.0 °C, where n=7.

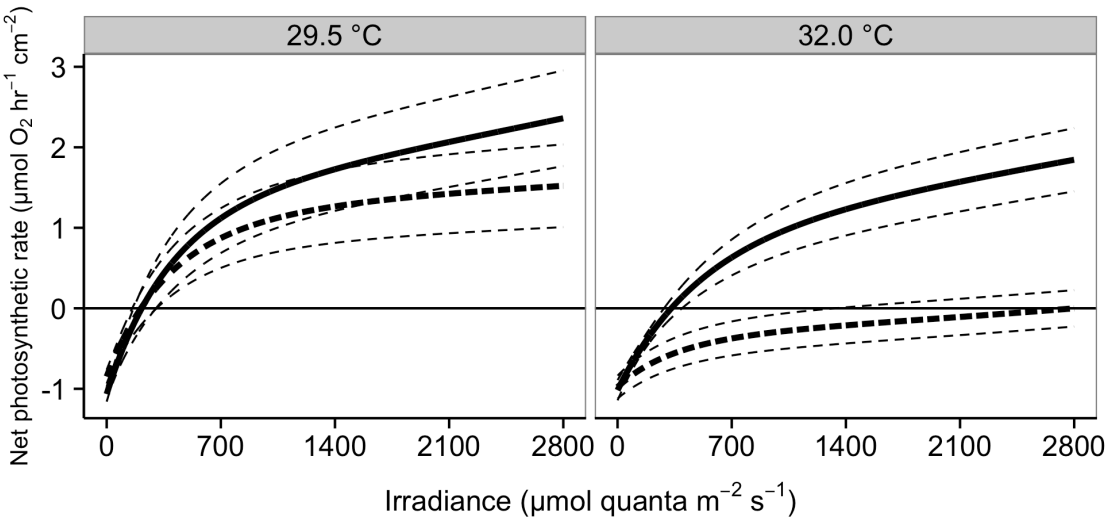

Figure 6. *Symbiodinium* gross photosynthetic rates (cm^{-2}) in encrusting and branching *Briareum asbestinum* at ambient and elevated temperatures.
Solid lines represent the average fitted photosynthetic rate cm^{-2} for either encrusting or branching *B. asbestinum*. Dashed lines represent ± standard error of the mean. See Table 4 for statistics and Table 5 for sample sizes.

Photosynthetic characteristics

Analysis of gross and net photosynthetic rates produced similar results, therefore we only describe the statistical results for gross photosynthetic rates (P; Table 4, Table 5). At both ambient and elevated temperature, encrusting fragments had higher *Symbiodinium* photosynthetic rates per surface area compared to the areal photosynthetic rates in branches (Figure 6, Table 5). The elevated temperature significantly reduced *Symbiodinium* photosynthetic rates per host surface area in both morphologies with a 16% and 59% reduction in encrusting fragments and branches, respectively (Table 4, Table 5). Consequently, at elevated temperature the difference in *Symbiodinium* photosynthesis cm^{-2} between the two morphologies increased, with *Symbiodinium* in encrusting fragments having nearly three times higher P cm^{-2} than *Symbiodinium* in branches. Elevated temperature caused a 5% and 65% reduction in *Symbiodinium* photosynthesis per chlorophyll *a* in encrusting fragments and branches,

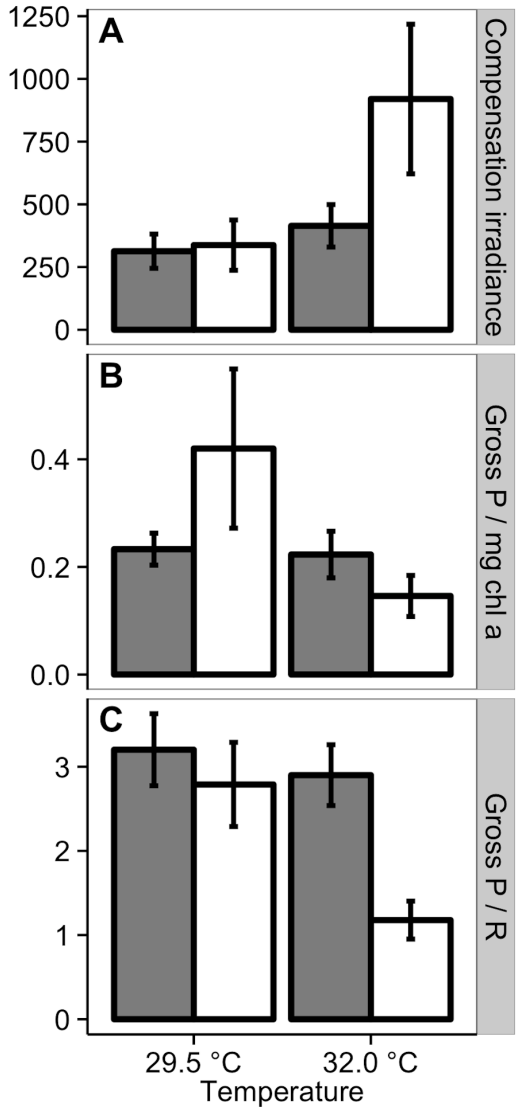

Figure 7. *Symbiodinium* photosynthetic characteristics in encrusting and branching *Briareum asbestinum* at ambient and elevated temperatures.
Compensation irradiance (E_c; µmol quanta m^{-2} s^{-1}) (A), the gross photosynthetic rate per mg chl *a* (µmol O_2 mg^{-1} chl *a*) (B), and the ratio of gross photosynthesis to respiration rate (gross P/R) (C) for *Symbiodinium* in encrusting (gray bars) and branching (white bars) *B. asbestinum* at 29.5 and 32.0 °C. Bar height and error bars represent the mean and standard error of the mean, respectively. See Table 4 for statistics and Table 5 for sample sizes.

respectively (Table 4). Photosynthetic rates per *Symbiodinium* cell were not significantly different between the two *B. asbestinum* morphologies and were not affected by elevated temperature (Table 4, Table 5).

The initial slope of the P-E curve, α chl^{-1} (also called the light utilization coefficient), and the compensation irradiance (E_c) were not significantly different between the two *B. asbestinum* morphologies. But, at elevated temperature, E_c was significantly greater than at ambient temperature, with E_c of encrusting fragments increasing by 30% and a three fold change in E_c of branches (Figure 7b, Table 5). Consequently, at the elevated temperature, E_c in encrusting fragments was half that found in branches. No significant differences were detected between *B. asbestinum* morphologies or temperature treatments in the saturation irradiance (E_k; Table 4, Table 5).

Respiration rates cm^{-2} were similar among *B. asbestinum* morphologies and temperature

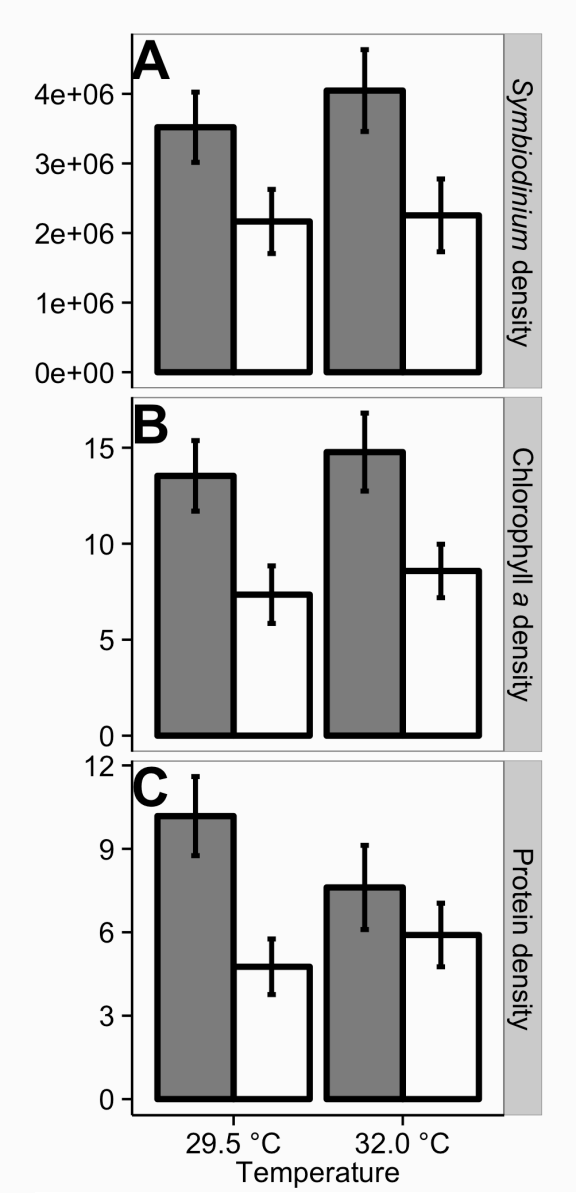

Figure 8. Parameters of *Symbiodinium* and their respective host encrusting and branching *Briareum asbestinum* at ambient and elevated temperatures.
Symbiodinium density (cells cm^{-2}) (A), chlorophyll *a* content (µg cm^{-2}) (B), and *B. asbestinum* protein content (mg cm^{-2}) (C) in encrusting (gray bars) and branching (white bars) at 29.5 and 32.0 °C. Bar height and error bars represent the mean and standard error of the mean, respectively. See Table 4 for statistics and Table 5 for sample sizes.

asbestinum morphology (Table 4).

treatments (Table 4, Table 5). On the other hand, the ratio of photosynthetic to respiratory rate, gross P/R, differed amongst *B. asbestinum* morphologies and temperature treatments (Figure 7c, Table 5). Encrusting fragments had significantly higher (15%) gross P/R than branches (Table 5). Compared to ambient temperature, elevated temperature significantly reduced gross P/R, with a 9% reduction in encrusting fragments and a 58% reduction of P/R in branches (Table 5) . As a result, encrusting fragments had more than double the gross P/R of branches at elevated temperature.

<u>*Symbiodinium* and chlorophyll densities</u>

Encrusting *B. asbestinum* fragments had significantly more *Symbiodinium* cells per host surface area than branches, with 59% and 74% more *Symbiodinium* cells cm^{-2} at ambient and elevated temperatures, respectively (Figure 8a, Table 4). Exposure to elevated temperature did not affect *Symbiodinium* density in either *B.*

Like *Symbiodinium* density, chlorophyll *a* density was significantly greater in encrusting fragments than in branches, by at least 42% at ambient and elevated temperatures (Figure 8b, Table 4). Encrusting fragments also had significantly more chl c_2 cm^{-2} than branches by at least 78% in both temperature treatments (Table 4, Table 5). The elevated temperature treatment did not significantly affect either chl *a* cm^{-2} or chl c_2 cm^{-2} in both morphologies (Table 5). The concentration of both chlorophylls per *Symbiodinium* cell and the ratio of chlorophyll a/c_2 did not significantly differ between *B. asbestinum* morphologies or temperature treatments (Table 4, Table 5).

Light absorption

Encrusting fragments had significantly lower estimated absorbance at 675 nm ($D_{e\,675}$) than branches by 13% at both ambient and elevated temperature (Table 4, Table 5). Compared to ambient temperature, elevated temperature significantly reduced $D_{e\,675}$ by 14% in both morphologies (Table 4). At both temperatures, in encrusting fragments, the specific absorption coefficient of chlorophyll *a* ($a^*_{chl\,a}$), was significantly lower (55%) compared to branches (Figure 9, Table 4).

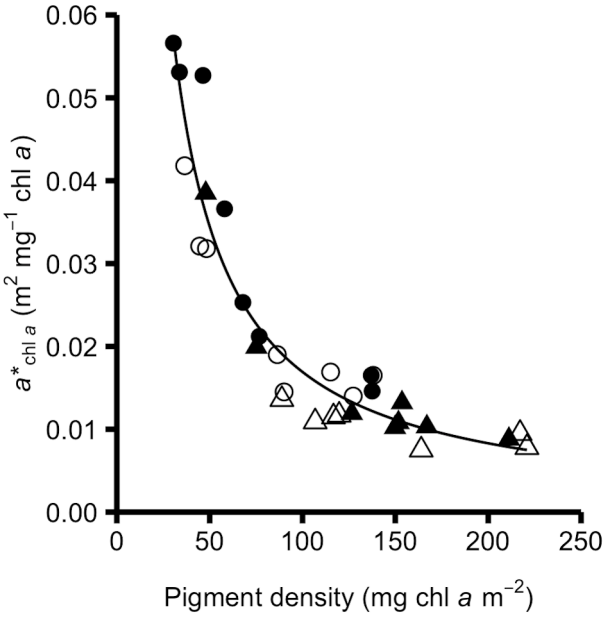

Figure 9. Chlorophyll *a* specific absorption, $a^*_{chl\,a}$, versus the pigment density of chlorophyll *a* at the end of the temperature treatments.
Triangles represent encrusting fragments while circles represent *B. asbestinum* branches. Filled symbols represent values at 29.5 °C, while open symbols represent values at 32.0 °C.

For both morphologies, exposure to elevated temperature reduced $a^*_{chl\ a}$ by 33% compared to $a^*_{chl\ a}$ at ambient temperature (Table 4). There was an exponential decrease in $a^*_{chl\ a}$ with increasing chlorophyll *a* density (Figure 9).

Briareum asbestinum protein content

Encrusting fragments had significantly more protein cm^{-2} than branches, with more than double the protein cm^{-2} of branches at ambient temperature and 29% more at elevated temperature (Figure 8c; Table 5). Exposure to elevated temperature did not significantly affect protein cm^{-2} (Table 5). Even though protein densities differed between morphologies, protein density did not correlate well with *Symbiodinium* density ($r(29)=0.23$, $P=0.207$), and thus protein density was not used to standardize photosynthetic parameters.

Briareum asbestinum polyp behavior

Since polyp behavior was not significantly different between sampling times or between temperatures (encrusting: $\chi^2<0.1$, $df=1$, $P=0.979$, $w<0.01$; branching: $\chi^2=0.2$, $df=1$, $P=0.696$, $w=0.06$), polyp behavior was pooled over the course of the experiment and between temperatures. The two *B. asbestinum* morphologies exhibited characteristic differences in polyp behavior at solar noon, when only 37% of encrusting fragments had expanded polyps compared to 59% of branches ($\chi^2=6.1$, $df=1$, $P=0.014$, $w=0.33$).

Table 4. *Symbiodinium* and host parameters in encrusting and branching *B. asbestinum* at ambient and elevated temperatures.

Means, standard deviations, and sample sizes for *B. asbestinum* branches and encrusting fragments sampled after exposure to 29.5 or 32.0 °C. *Symbiodinium* identities associated with each morphology are listed in parentheses. Parameters include the density of *Symbiodinium* cells (cells cm^{-2}), protein content (mg cm^{-2}), chlorophyll (chl) *a* and c_2 (µg chl cm^{-2}, pg chl $cell^{-1}$), estimated absorbance by chlorophyll *a* ($D_{e\ 675}$), photosynthetic rates (P; µmol O_2 hr^{-1}), respiration rates (R; µmol O_2 hr^{-1}), the ratio of gross photosynthesis to respiration (gross P/R), and characteristics of the light-limited portion of photosynthesis-irradiance curves (α: photosynthetic efficiency; E_c: compensation irradiance; E_k: saturation irradiance). # indicates where n=8, $ indicates where n=6, and ^ indicates where n=5.

	29.5 °C		**32.0 °C**	
	Encrusting (B19; n=7)	**Branching (B21; n=7)**	**Encrusting (B19; n=7)**	**Branching (B21; n=8)**
Symbiodinium				
cells cm^{-2} *10^6	3.52 ± 1.43 #	2.17 ± 1.30 #	4.05 ± 1.56	2.25 ± 1.48
µg chl *a* cm^{-2}	13.53 ± 5.20 #	7.35 ± 4.24 #	14.77 ± 5.37	8.58 ± 3.94
µg chl c_2 cm^{-2}	3.97 ± 2.05 #	2.23 ±1.19	4.76 ± 2.53	2.53 ± 0.81
pg chl *a* $cell^{-1}$	4.03 ± 1.12 #	4.72 ± 3.23 #	3.83 ± 1.03	4.36 ± 1.92
pg chl c_2 $cell^{-1}$	1.11 ± 0.39 #	1.58 ± 1.00	1.25 ± 0.61	1.36 ± 0.61
chl a/c_2	3.73 ± 0.86 #	3.31 ± 0.39	3.85 ± 2.19	3.34 ± 0.86
$D_{e\ 675}$	0.74 ± 0.08 #	0.85 ± 0.13 #	0.63 ± 0.14	0.73 ± 0.14
gross P cm^{-2}	3.43 ± 1.70	2.37 ± 1.44	2.86 ± 1.19	0.97 ± 0.40
net P cm^{-2}	2.36 ± 1.57	1.52 ± 1.36	1.85 ± 1.04	0.00 ± 0.64
gross P $cell^{-1}$ *10^6	0.93 ± 0.45	1.47 ± 1.64	0.87 ± 0.61	0.60 ± 0.40
net P $cell^{-1}$ *10^6	0.64 ± 0.41	1.01 ± 1.36	0.59 ± 0.47	0.17 ± 0.32
gross P $µg^{-1}$ chl *a*	0.23 ± 0.09	0.42 ± 0.39	0.22 ± 0.12	0.15 ± 0.11
net P $µg^{-1}$ chl *a*	0.16 ± 0.08	0.29 ±0.33	0.15 ± 0.09	0.14 ± 0.09
R cm^{-2}	-1.07 ± 0.25	-0.85 ± 0.23	-1.02 ± 0.33	-0.98 ± 0.40
gross P/R	3.20 ± 1.13	2.79 ± 1.32	2.90 ± 0.96	1.18 ± 0.64
α chl^{-1} *10^{-3} (P $µg^{-1}$ chl *a*)	0.43 ± 0.27	1.02 ± 1.26	0.31 ± 0.17	0.40 ± 0.26
α cm^{-2} *10^{-2} (P cm^{-2})	0.65 ± 0.47	0.53 ± 0.37	0.41 ± 0.20 $	0.28 ± 0.18
E_c	313 ± 181	337 ± 266	414 ± 224	920 ± 667 ^
E_k	614 ± 161	501 ± 200	844 ± 602	486 ± 261
Briareum host				
mg protein cm^{-2}	10.18 ± 4.02 #	4.75 ± 2.83 #	7.61 ± 4.01	5.90 ± 3.23

Table 5. Linear mixed model results. Degrees of freedom (df), F statistics (F), and P values (P) for a linear mixed model using *Briareum asbestinum* morphology (encrusting, branching) and temperature treatment (29.5 °C, 32.0 °C) as factors. For each parameter, factors with P<0.05 are indicated by *.

	Morphology			**Temperature**			**Morph.*Temp.**	
	df error	**F (df=1)**	**P**	**df error**	**F (df=1)**	**P**	**F (df=1)**	**P**
Symbiodinium								
cells cm^{-2}	14.3	7.8	**0.01**	14.1	0.4	0.53	0.2	0.65
chl *a* cm^{-2}	14.1	10.2	**0.01**	13.7	1.0	0.34	<0.1	0.95
chl c_2 cm^{-2}	14.5	4.4	**0.05**	13.5	1.3	0.27	<0.1	0.98
chl *a* $cell^{-1}$	14.2	0.4	0.55	13.6	0.3	0.62	0.1	0.80
chl c_2 $cell^{-1}$	14.2	0.3	0.59	13.6	0.2	0.66	0.3	0.62
chl a/c_2	13.4	0.1	0.80	12.4	1.8	0.20	1.3	0.28
$a^*_{\text{chl a}}$	14.0	21.4	**<0.01**	13.9	4.7	**0.05**	<0.1	0.87
gross P cm^{-2}	14.3	5.5	**0.03**	13.7	8.3	**0.01**	<0.1	0.99
gross P $cell^{-1}$	14.4	0.3	0.57	12.9	5.2	**0.04**	0.2	0.64
gross P chl^{-1}	13.9	0.3	0.57	12.1	8.5	**0.01**	<0.1	0.89
α chl^{-1}	14.0	1.3	0.28	13.4	5.4	**0.04**	0.4	0.55
α cm^{-2}	24.0	3.0	0.10	24.0	7.8	**0.01**	24.0	0.42
E_c	13.55	3.6	0.08	13.3	6.4	**0.02**	3.1	0.10
E_k	24.0	2.3	0.14	24.0	0.2	0.69	1.5	0.23
R cm^{-2}	14.3	2.0	0.18	13.6	1.3	0.27	0.7	0.42
24 h g P/R	13.0	25.0	**<0.01**	13.0	5.1	**0.04**	0.1	0.72
Briareum host								
protein cm^{-2}	14.2	7.1	**0.02**	14.1	0.1	0.75	2.1	0.17

Discussion

The morphology of sedentary organisms is influenced by both the organism's genetic makeup and the environment it inhabits. In the marine environment, organisms from the same species, found in locations with different environmental conditions, such as flow rates or light levels, may exhibit different morphologies. The influence of the environment on these different forms can be demonstrated through reciprocal transplant experiments (Todd 2008). For example, transplantation of branching colonies of the octocoral *Briareum asbestinum* from shallow to deep depth induced changes in branch dimensions, skeletal composition, and polyp density (West et al. 1993).

On the other hand, sometimes the same species can exhibit different morphologies in the same habitat, such as the scleractinian coral *Montipora capitata* which exhibits plating and branching morphologies that co-occur at the same depth (Padilla-Gamiño et al. 2012). Similarly, the octocoral *B. asbestinum* in shallow Caribbean reefs exhibits either a branching or encrusting morphology (Brazeau and Lasker 1992; Bilewitch et al. 2010; this study). The evolutionary or ecological processes that maintain two distinct morphologies side by side are unclear. Since both scleractinian corals and many octocorals have an obligatory mutualistic symbiosis with dinoflagellates belonging to the genus *Symbiodinium*, the host morphology may be influenced by its resident symbionts and their photosynthesis within the host. Or, conversely, the host morphology may affect which symbionts it associates with.

In *B. asbestinum*, previous studies reported that the encrusting morphology associates with only *Symbiodinium* type B1, or B1 and B19 (Hannes et al. 2009; Poland et al. 2013). Branching *B. asbestinum* colonies have been documented hosting either *Symbiodinium* type B1,

B19, B33, or even C types C1, and C3L (Goulet and Coffroth 2004; Goulet et al. 2008; Finney et al. 2010). In our study, we found a clear symbiont distinction between the two *B. asbestinum* morphologies whereby the encrusting morphology hosted only *Symbiodinium* type B19 while the branching morphology associated only with *Symbiodinium* type B21. Sampling *B. asbestinum* colonies in different geographic locations such as the Florida Keys, USA (Hannes et al. 2009; Poland et al. 2013), Belize, and Barbados (Finney et al. 2010) may explain the differences in symbiont identity between the studies. Nevertheless, having two distinct symbionts in the two different morphologies in our study site enabled us to compare the symbiosis in the two host morphologies without confounding the comparison with multiple host-symbiont genotypic combinations.

The *Symbiodinium* in *B. asbestinum* not only differed genetically but also morphologically. *Symbiodinium* B19 found in encrusting *B. asbestinum* was larger than the *Symbiodinium* B21 found in the branching morphology. The clade B types in *Madracis pharensis* also exhibited characteristic cell sizes which were independent of irradiance exposure (Frade et al. 2008b), suggesting that *Symbiodinium* cell size may be largely genetically determined (LaJeunesse 2001). Alternatively, the different diameters of B19 and B21 *Symbiodinium* may be related to the tissue characteristics of their hosts. Encrusting fragments had more protein cm^{-2}, which may have reduced the light available for the symbionts (Kaniewska et al. 2011) and triggered a photoacclimatory increase in *Symbiodinium* cell size (Lesser and Shick 1989; Thompson et al. 1991).

Even though the B19 *Symbiodinium* in encrusting *B. asbestinum* were larger, their size did not lead to fewer symbionts per unit surface area of the host. In fact, the opposite was the

case, whereby at ambient temperature, encrusting *B. asbestinum* had 54% more symbionts per colony surface area than the branching *B. asbestinum*. On the other hand, the amount of chlorophyll per *Symbiodinium* cell did not significantly differ between B19 and B21. Consequently, encrusting *B. asbestinum* had significantly more chlorophyll density compared to the branching morphology.

Although the two *B. asbestinum* morphologies occur side by side at the same depth, irradiance exposure differed dramatically. Polyps in the horizontally oriented encrusting morphology were exposed to nearly three times greater irradiance at solar noon than the polyps of the vertical branches, which likely contributed to the low effective quantum yield, high excitation pressure over photosystem II, and perhaps the contracted polyps in encrusting fragments at solar noon. Due to the vertical orientation of branches, expanded polyps of branching *B. asbestinum* experienced much lower irradiance than those in encrusting fragments, which may have led to the high effective quantum yield as well as the high pigment absorption efficiency by chlorophyll *a*. However, like the vertical orientation of branches, the tissues and protein of encrusting *B. asbestinum* could have also reduced irradiance levels, and resulted in similar irradiance exposure for *Symbiodinium* within encrusting and branching *B. asbestinum* (Kaniewska et al. 2011; Dimond et al. 2012).

Symbiodinium in encrusting fragments had lower estimated absorbance at 675 nm and chlorophyll *a* specific absorption than branches, which may have helped reduce excessive light absorption. Lower chl *a* specific absorption in encrusting *B. asbestinum* may be in part due to its association with the larger *Symbiodinium*, type B19. In phytoplankton, cells with greater volume can have reduced chlorophyll specific absorption (Fujiki and Taguchi 2002), potentially due to

reduced cellular chlorophyll packaging.

Hosting genetically distinct symbionts of a particular size, combined with host orientation and tissue characteristics, may have affected the photosynthetic parameters in the symbiosis. The potentially similar irradiance exposure may explain the similar photoacclimation by their *Symbiodinium* at ambient temperature, as indicated by cellular chlorophyll concentrations and the initial slope of the PE curves. Furthermore, under ambient conditions, E_c, E_k and photosynthesis per *Symbiodinium* cell were also not significantly different between the two *B. asbestinum* morphologies. On the other hand, because encrusting *B. asbestinum* fragments had significantly more *Symbiodinium* in the branching *B. asbestinum* morphology, encrusting fragments had significantly higher photosynthetic rates and chlorophyll a density per host surface area. In addition, although in both *B. asbestinum* morphologies had similar respiration rates, due to the higher photosynthetic rates, the encrusting morphology had significantly higher P/R ratios.

In many scleractinian coral species, short term exposure to elevated seawater temperature can lead to a drastic decline in *Symbiodinium* densities and/or chlorophyll *a* (Fitt et al. 2009), commonly called coral bleaching (Fitt et al. 2001; Glynn et al. 2001; Weis 2008). In our study, exposing *B. asbestinum* to seven days of elevated temperatures of 32.0 °C did not cause a significant change in symbiont density or chlorophyll content in either the encrusting or branching morphologies. Thus, both *B. asbestinum* morphologies can withstand a short period of thermal stress without a breakdown of their symbiosis with clade B symbionts. Our findings corroborate field observations. In the Bahamas during a thermal event in which seawater temperatures reached 33°C, 13 gorgonian species were monitored and branching *B. asbestinum* did not bleach nor exhibit necrotic tissue (Lasker 2005). Another Caribbean octocoral, *Eunicea*

tourneforti, is also relatively robust to elevated temperature and maintained symbiont densities after a two week exposure at +2.5 °C (Drohan et al. 2005).

Bleaching in *B. asbestinum* has been occasionally reported. Branching *B. asbestinum* visually bleached following a period of elevated temperature in 1983, but the number of bleached colonies was not reported (Lasker et al. 1984). Bleaching and subsequent mortality in *B. asbestinum* could be a consequence of disease (Harvell et al. 2001). The branching *B. asbestinum* in those studies could have hosted *Symbiodinium* C types since octocorals that harbor clade C *Symbiodinium* may be more susceptible to bleaching (Goulet and Coffroth 2004). Encrusting colonies visually bleached following a period of elevated temperature in 2005 (Prada et al. 2010). Perhaps the thermal histories (Middlebrook et al. 2008) or the symbiont types associated with these *B. asbestinum* colonies increased their thermal sensitivity compared to those studied here.

In our study, the effect of the elevated seawater temperature on the branching morphology was larger than on the encrusting morphology. Multiple factors could have contributed to the greater susceptibility of *B. asbestinum* branches to elevated temperature. The B21 symbiont in branches may be more susceptible to thermal stress than the B19 symbiont in encrusting fragments, as photosynthetic characteristics differ among clade B *Symbiodinium* types (Frade et al. 2008a; Hennige et al. 2009). In addition, the greater chlorophyll *a* specific absorption in branches may have contributed to higher thermal sensitivity (Jones and Berkelmans 2012), as each chlorophyll molecule absorbed more energy in branches compared to encrusting fragments, leading to increased production of toxic oxygen radicals by damaged photosystem II reaction centers (Lesser et al. 1990). Higher light absorption and photochemical efficiencies at

solar noon in branches may have exacerbated light-induced damage to *Symbiodinium* cells in branching *B. asbestinum*.

Conversely, the B19 *Symbiodinium* within the encrusting *B. asbestinum* maintained photosynthetic rates comparable to those at 29.5 °C. The larger *Symbiodinium* densities or greater tissue thickness in encrusting fragments may have mediated the effects of thermal stress on its *Symbiodinium*. Our findings concur with observations from scleractinian corals, where branching species can be more sensitive to elevated temperature than mounding or encrusting species (Loya et al. 2001; van Woesik et al. 2011). Branching species may be more sensitive to elevated temperatures due to thinner tissues (Loya et al. 2001), higher surface area to volume ratios (Fujioka 1999), or lower mass transfer than mounding or encrusting species (van Woesik et al. 2012).

Our study demonstrates that, although residing side by side on the same reef, at the same depth, encrusting and branching morphologies of *B. asbestinum* differ in their protein content, polyp activity, the genetic composition of their *Symbiodinium* and numerous photosynthetic parameters, including different responses to elevated temperature. It beckons to question whether these two *B. asbestinum* morphologies indeed represent one species. For example, in the scleractinian genus *Pocillopora*, association with distinct symbionts coincided with genetic breaks between cryptic coral species (Pinzon and LaJeunesse 2011). Diverging lineages have been identified within the Caribbean octocoral *Eunicea flexuosa* (Prada et al. 2008; Prada and Hellberg 2013).

For *B. asbestinum,* past studies raised conflicting conclusions. The two morphologies of *B. asbestinum* have been considered distinct genera (Cairns 1977); distinct species within the

genus *Briareum* (Sánchez and Wirshing 2005); or as members of the same species, *B. asbestinum* (Bayer 1961; Bilewitch et al. 2010). Genetic analyses have also produced mixed interpretations. One study reported differences in allele frequencies between colony morphologies and concluded that gene flow between morphologies is restricted (Brazeau and Harvell 1994). On the other hand, a second study found identical mitochondrial *msh1* sequences in both morphologies, surmising that genetic differentiation between morphologies was small or very recent (Bilewitch et al. 2010). In our study, both encrusting and branching *B. asbestinum* colonies had identical *msh1* sequences and these matched the sequence recovered by Bilewitch et al. (2010). The lack of variation in *msh1* sequence suggests that less genetic differentiation has occurred between *B. asbestinum* morphologies than between other *Briareum* species (*B. asbestinum*, *B. habrum* [GenBank:GU356010], *B. violaceum* [GenBank:KF915571]). Looking at other molecular markers will hopefully resolve the taxonomic questions.

CONCLUSION

These two studies emphasized the effects of colony morphology and host identity on symbiont physiology. In Chapter I, *Pterogorgia anceps* and *Pseudoplexaura wagenaari* both harbored type B1 *Symbiodinium*, however the photosynthetic characteristics of each symbiosis differed. On the other hand, *Pseudoplexaura porosa* and *Pseudoplexaura wagenaari* harbored distinct *Symbiodinium* types, but the photosynthetic characteristics of the congeneric species were quite similar. The observed photosynthetic differences between Caribbean gorgonian symbioses may be related to host morphology or host physiology rather than physiological variation of their respective symbionts.

In Chapter II, the two morphologies of *Briareum asbestinum* harbor distinct *Symbiodinium* types that may have contributed to the photosynthetic characteristics of each morphology. Association with particular symbionts can confer robustness to elevated temperature, and may have contributed to the relative thermal tolerance of the encrusting/B19 symbiosis compared to the branching/B21 symbiosis. Despite thermal impairment of photosynthesis, neither of the *B. asbestinum* morphologies bleached, which indicates that these symbioses can withstand short term (~1 week) exposure to elevated temperatures. In general, scant data exist regarding the frequency or intensity of coral bleaching in Caribbean gorgonians, but this study on *B. asbestinum* suggests that gorgonian symbioses can be maintained at elevated temperature, even when *Symbiodinium* photosynthesis is compromised.

The octocoral *Briareum asbestinum* displays two unique morphotypes which co-occur at

the same depth in the same habitat on shallow Caribbean reefs. Our findings demonstrate numerous differences in both host parameters and *Symbiodinium* physiology within these two discrete morphologies, as well as that elevated temperature more negatively affects the branching morphology. Although debate still exists as to whether these two morphologies represent one species, *B. asbestinum* provides an opportunity to investigate variation due to morphology uncoupled from environmental parameters that may lead to differences between morphologies.

LIST OF REFERENCES

Aizenberg J, Sundar VC, Yablon AD, Weaver JC, Chen G (2004) Biological glass fibers: correlation between optical and structural properties. Proc Natl Acad Sci USA 101:3358-3363
Baker DM, Kim K, Andras JP, Sparks JP (2011) Light-mediated ^{15}N fractionation in Caribbean gorgonian octocorals: implications for pollution monitoring. Coral Reefs 30:709-717
Bayer FM (1961) The shallow-water Octocorallia of the West Indian region. Studies on the Fauna of Curaçao and other Caribbean Islands 12:1-428
Bilewitch JP, Coates KA, Currie DC, Trapido-Rosenthal HG (2010) Molecular and morphological variation supports monotypy of the octocoral *Briareum* Blainville, 1830 (Octocorallia: Alcyonacea) in the Western Atlantic. P Biol Soc Wash 123:93-112
Borell EM, Bischof K (2008) Feeding sustains photosynthetic quantum yield of a scleractinian coral during thermal stress. Oecologia 157:593-601
Brading P, Warner ME, Smith DJ, Suggett DJ (2013) Contrasting modes of inorganic carbon acquisition amongst *Symbiodinium* (Dinophyceae) phylotypes. New Phytol 200:432-442
Brazeau DA, Lasker HR (1992) Growth rates and growth strategy in a clonal marine invertebrate, the Caribbean octocoral *Briareum asbestinum*. Biol Bull 183:269-277
Brazeau DA, Harvell CD (1994) Genetic structure of local populations and divergence between growth forms in a clonal invertebrate, the Caribbean octocoral *Briareum asbestinum*. Mar Biol 119:53-60
Bricaud A, Babin M, Morel A, Claustre H (1995) Variability in the chlorophyll-specific absorption coefficients of natural phytoplankton: Analysis and parameterization. J Geophys Res-Oceans 100:13321-13332
Brown BE (1997) Coral bleaching: causes and consequences. Coral Reefs 16:S129-S138
Brümmer F, Pfannkuchen M, Baltz A, Hauser T, Thiel V (2008) Light inside sponges. J Exp Mar Biol Ecol 367:61-64
Bruno JF, Edmunds PJ (1997) Clonal variation for phenotypic plasticity in the coral *Madracis mirabilis*. Ecology 78:2177-2190
Burkholder PR, Burkholder LM (1960) Photosynthesis in some Alcyonacean corals. Am J Bot 47:866-872
Cairns SD (1977) Guide to the commoner shallow-water gorgonians of South Florida, the Gulf of Mexico, and the Caribbean region. University of Miami Sea Grant Field Guide Series 6:1-74
Cary LR (1918) The Gorgonaceae as a factor in the formation of coral reefs. Pap. Tortugas Lab
Chang W-L, Chi K-J, Fan T-Y, Dai C-F (2007) Skeletal modification in response to flow during growth in colonies of the sea whip, *Junceella fragilis*. J Exp Mar Biol Ecol 347:97-108
Colvard NB, Edmunds PJ (2011) Decadal-scale changes in abundance of non-scleractinian invertebrates on a Caribbean coral reef. J Exp Mar Bio Ecol 397:153-160
Dahlgren EJ (1989) Gorgonian community structure and reef zonation patterns on Yucatan coral reefs. Bull Mar Sci 45:678-696
Day T, Nagel L, van Oppen MJH, Caley MJ (2008) Factors affecting the evolution of bleaching resistance in corals. Am Nat 171:E72-88
Dimond JL, Holzman BJ, Bingham BL (2012) Thicker host tissues moderate light stress in a

cnidarian endosymbiont. J Exp Biol 215:2247-2254
Drohan AF, Thoney DA, Baker AC (2005) Synergistic effect of high temperature and ultraviolet-B radiation on the gorgonian *Eunicea tourneforti* (Octocorallia : Alcyonacea : Plexauridae). Bull Mar Sci 77:257-266
Dubinsky Z, Falkowski PG (2011) Light as a source of information and energy in zooxanthellate corals. In: Dubinsky Z, Stambler N (eds) Coral reefs: an ecosystem in transition. Springer Science+Business Media, Dordrecht, pp107-118
Dubinsky Z, Falkowski PG, Porter JW, Muscatine L (1984) Absorption and utilization of radiant energy by light-and shade-adapted colonies of the hermatypic coral *Stylophora pistillata*. Proc R Soc Lond B Biol Sci 222:203-214
Duchassaing P, Michelotti J (1860) Mémoire sur les coralliaires des Antilles. Memorie della Reale Accademia delle Scienze di Torino Serie seconda 19:279-265
Edmunds PJ, Elahi R (2007) The demographics of a 15-year decline in cover of the Caribbean reef coral *Montastraea annularis*. Ecol Monogr 77:3-18
Edmunds PJ, Putnam HM, Nisbet RM, Muller EB (2011) Benchmarks in organism performance and their use in comparative analyses. Oecologia 167:379-390
Enríquez S, Méndez ER, Iglesias-Prieto R (2005) Multiple scattering on coral skeletons enhances light absorption by symbiotic algae. Limnol Oceanogr:1025-1032
Ezzat L, Merle P-L, Furla P, Buttler A, Ferrier-Pages C (2013) The response of the Mediterranean gorgonian *Eunicella singularis* to thermal stress is independent of its nutritional regime. PLoS ONE 8:e64370
Fabricius KE, Klumpp DW (1995) Widespread mixotrophy in reef-inhabiting soft corals: the influence of depth, and colony expansion and contraction on photosynthesis. Mar Ecol Prog Ser 125:195-204
Farrant PA, Borowitzka MA, Hinde R, King RJ (1987) Nutrition of the temperate Australian soft coral *Capnella gaboensis* 1. Photosynthesis and carbon fixation. Mar Biol 95:565-574
Ferrier-Pages C, Hoogenboom MO, Houlbreque F (2011) The role of plankton in coral trophodynamics. In: Dubinsky Z, Stambler N (eds) Coral reefs: an ecosystem in transition. Springer Science+Business Media, Dordrecht, pp215-229
Ferrier-Pages C, Tambutté E, Zamoum T, Segonds N, Merle P-L, Bensoussan N, Allemand D, Garrabou J, Tambutté S (2009) Physiological response of the symbiotic gorgonian *Eunicella singularis* to a long-term temperature increase. J Exp Biol 212:3007-3015
Finney JC, Pettay DT, Sampayo EM, Warner ME, Oxenford HA, LaJeunesse TC (2010) The relative significance of host–habitat, depth, and geography on the ecology, endemism, and speciation of coral endosymbionts in the genus *Symbiodinium*. Microb Ecol 60:250-263
Fitt WK, Cook CB (2001) Photoacclimation and the effect of the symbiotic environment on the photosynthetic response of symbiotic dinoflagellates in the tropical marine hydroid *Myrionema amboinense*. J Exp Mar Bio Ecol 256:15-31
Fitt WK, McFarland FK, Warner ME, Chilcoat GC (2000) Seasonal patterns of tissue biomass and densities of symbiotic dinoflagellates in reef corals and relation to coral bleaching. Limnol Oceanogr 45:677-685

Fitt WK, Brown BE, Warner ME, Dunne RP (2001) Coral bleaching: interpretation of thermal tolerance limits and thermal thresholds in tropical corals. Coral Reefs 20:51-65
Fitt WK, Gates RD, Hoegh-Guldberg O, Bythell JC, Jatkar A, Grottoli AG, Gomez M, Fisher PL, LaJeunesse TC, Pantos O, Iglesias-Prieto R, Franklin DJ, Rodrigues LJ, Torregiani JM, van Woesik R, Lesser MP (2009) Response of two species of Indo-Pacific corals, *Porites cylindrica* and *Stylophora pistillata*, to short-term thermal stress: The host does matter in determining the tolerance of corals to bleaching. J Exp Mar Biol Ecol 373:102-110
Forsman ZH, Barshis DJ, Hunter CL, Toonen RJ (2009) Shape-shifting corals: molecular markers show morphology is evolutionarily plastic in *Porites*. BMC Evol Biol 9:45
Frade PR, Bongaerts P, Winkelhagen AJS, Tonk L, Bak RPM (2008a) In situ photobiology of corals over large depth ranges: A multivariate analysis on the roles of environment, host, and algal symbiont. Limnol Oceanogr 53:2711-2723
Frade PR, Englebert N, Faria J, Visser PM, Bak RPM (2008b) Distribution and photobiology of *Symbiodinium* types in different light environments for three colour morphs of the coral *Madracis pharensis*: is there more to it than total irradiance? Coral Reefs 27:913-925
Fujiki T, Taguchi S (2002) Variability in chlorophyll *a* specific absorption coefficient in marine phytoplankton as a function of cell size and irradiance. J Plankton Res 24:859-874
Fujioka Y (1999) Mass destruction of the hermatypic corals during a bleaching event in Ishigaki Island, southwestern Japan. Galaxea, JCRS 1:41-50
Gardner TA, Côte IM, Gill JA, Grant A, Watkinson AR (2003) Long-term region-wide declines in Caribbean corals. Science 301:958-960
Glynn PW, Mate JL, Baker AC, Calderon MO (2001) Coral bleaching and mortality in Panama and Ecuador during the 1997--98 El Nino--Southern Oscillation event: spatial/temporal patterns and comparisons with the 1982--1983 event. Bull Mar Sci 69:79-109
Goiran C, Allemand D, Galgani I (1997) Transient Na^+ stress in symbiotic dinoflagellates after isolation from coral-host cells and subsequent immersion in seawater. Mar Biol 129:581-589
Goiran C, Al-Moghrabi SM, Allemand D, Jaubert J (1996) Inorganic carbon uptake for photosynthesis by the symbiotic coral/dinoflagellate association I. Photosynthetic performances of symbionts and dependence on sea water bicarbonate. J Exp Mar Bio Ecol 199:207-225
Goldberg WM (1973) The ecology of the coral-octocoral communities off the southeast Florida coast: geomorphology, species composition, and zonation. Bull Mar Sci 23:465-488
Goldberg WM, Benayahu Y (1987a) Spicule formation in the gorgonian coral *Pseudoplexaura flagellosa*. 1: Demonstration of intracellular and extracellular growth and the effect of ruthenium red during decalcification. Bull Mar Sci 40:287-303
Goldberg WM, Benayahu Y (1987b) Spicule formation in the gorgonian coral *Pseudoplexaura flagellosa*. 2: Calcium localization by antimonate precipitation. Bull Mar Sci 40:304-310
Gorbunov MY, Kolber ZS, Lesser MP, Falkowski PG (2001) Photosynthesis and photoprotection in symbiotic corals. Limnol Oceanogr 46:75-85
Goulet TL (2006) Most corals may not change their symbionts. Mar Ecol Prog Ser 321:1-7

Goulet TL, Coffroth MA (2004) The genetic identity of dinoflagellate symbionts in Caribbean octocorals. Coral Reefs 23:465-472
Goulet TL, Cook CB, Goulet D (2005) Effect of short-term exposure to elevated temperatures and light levels on photosynthesis of different host-symbiont combinations in the *Aiptasia pallida*/*Symbiodinium* symbiosis. Limnol Oceanogr 50:1490-1498
Goulet TL, Simmons C, Goulet D (2008) Worldwide biogeography of *Symbiodinium* in tropical octocorals. Mar Ecol Prog Ser 355:45-58
Grajales A, Aguilar C, Sánchez JA (2007) Phylogenetic reconstruction using secondary structures of Internal Transcribed Spacer 2 (ITS2, rDNA): finding the molecular and morphological gap in Caribbean gorgonian corals. BMC Evol Biol 7:90
Gutierrez-Rodriguez C, Barbeitos MS, Sánchez JA, Lasker HR (2009) Phylogeography and morphological variation of the branching octocoral *Pseudopterogorgia elisabethae*. Mol Phylogen Evol 50:1-15
Hannes AR, Barbeitos MS, Coffroth MA (2009) Stability of symbiotic dinoflagellate type in the octocoral *Briareum asbestinum*. Mar Ecol Prog Ser 391:65-72
Harvell CD, Kim K, Quirolo C, Weir J, Smith GW (2001) Coral bleaching and disease: contributors to 1998 mass mortality in *Briareum asbestinum* (Octocorallia, Gorgonacea). Hydrobiologia 460:97-104
Hennige SJ, Suggett DJ, Warner ME, McDougall KE, Smith DJ (2009) Photobiology of *Symbiodinium* revisited: bio-physical and bio-optical signatures. Coral Reefs 28:179-195
Hoogenboom MO, Connolly SR, Anthony KRN (2008) Interactions between morphological and physiological plasticity optimize energy acquisition in corals. Ecology 89:1144-1154
Hothorn T, Bretz F, Westfall P (2008) Simultaneous Inference in General Parametric Models. Biom J 50:346-363
Houlbreque F, Ferrier-Pages C (2009) Heterotrophy in tropical scleractinian corals. Biol Rev 84:1-17
Huelsenbeck JP, Ronquist F (2001) MRBAYES: Bayesian inference of phylogenetic trees. Bioinformatics (Oxford, England) 17:754-755
Hughes TP (1994) Catastrophes, phase shifts, and large-scale degradation of a Caribbean coral reef. Science 265:1547-1551
Iglesias-Prieto R, Trench RK (1994) Acclimation and adaptation to irradiance in symbiotic dinoflagellates. 1. Responses of the photosynthetic unit to changes in photon flux density. Mar Ecol Prog Ser 113:163-175
Iglesias-Prieto R, Beltran VH, LaJeunesse TC, Reyes-Bonilla H, Thomé PE (2004) Different algal symbionts explain the vertical distribution of dominant reef corals in the eastern Pacific. Proc. R. Soc. Lond. B 271:1757-1763
Imbs AB, Dautova TN (2008) Use of lipids for chemotaxonomy of octocorals (Cnidaria: Alcyonaria). Russ J Mar Biol 34:174-178
IPCC, 2007: Summary for Policymakers. In: Solomon S, Qin D, Manning M, Chen Z, Marquis M, Averyt KB, Tignor M, Miller HL (eds) Climate Change 2007: The Physical Science Basis Contribution of Working Group I to the Fourth Assessment Report of the Intergovernmental Panel on Climate Change. Cambridge University Press, Cambridge,

United Kingdom and New York, NY USA, pp1-18
Jeffrey SW, Humphrey GF (1975) New spectrophotometric equations for determining chlorophylls *a*, *b*, c_1 and c_2 in higher plants, algae and natural phytoplankton. Biochem Physiol Pflanz (BPP) 167:191-194
Jeong HJ, Lee SY, Kang NS, Yoo YD, Lim AS, Lee MJ, Kim HS, Yih W, Yamashita H, LaJeunesse TC (2014) Genetics and morphology characterize the dinoflagellate *Symbiodinium voratum*, n. sp., (Dinophyceae) as the sole representative of *Symbiodinium* clade E. J Eukaryot Microbiol 61:75-94
Jones A, Berkelmans R (2012) The photokinetics of thermo-tolerance in *Symbiodinium*. Photokinetics of heat tolerance in reef corals 33:490-498
Jones RJ, Hoegh-Guldberg O, Larkum AWD, Schreiber U (1998) Temperature-induced bleaching of corals begins with impairment of the CO2 fixation mechanism in zooxanthellae. Plant Cell Environ 21:1219-1230
Kaniewska P, Anthony KRN, Hoegh-Guldberg O (2008) Variation in colony geometry modulates internal light levels in branching corals, *Acropora humilis* and *Stylophora pistillata*. Mar Biol 155:649-660
Kaniewska P, Magnusson SH, Anthony KRN, Reef R, Kühl M, Hoegh-Guldberg O (2011) Importance of macro- versus microstructure in modulating light levels inside coral colonies. J Phycol 47:846-860
Kanwisher JW, Wainwright SA (1967) Oxygen balance in some reef corals. Biol Bull 133:378-390
Khalesi MK, Beeftink HH, Wijffels RH (2011) Energy budget for the cultured, zooxanthellate octocoral *Sinularia flexibilis*. Mar Biotechnol 13:1092-1098
Kim E, Lasker HR, Coffroth MA, Kim K (2004) Morphological and genetic variation across reef habitats in a broadcast-spawning octocoral. Hydrobiologia 530-531:423-432
Kinzie I, Robert A (1973) The zonation of West Indian gorgonians. Bull Mar Sci 23:93-155
Kühl M, Cohen Y, Dalsgaard T, Jørgensen BB, Revsbech NP (1995) Microenvironment and photosynthesis of zooxanthellae in scleractinian corals studied with microsensors for O2, pH and light. Mar Ecol Prog Ser 117:159-172
LaJeunesse TC (2001) Investigating the biodiversity, ecology, and phylogeny of endosymbiotic dinoflagellates in the genus *Symbiodinium* using the ITS region: in search of a "species" level marker. J Phycol 37:866-880
LaJeunesse TC (2002) Diversity and community structure of symbiotic dinoflagellates from Caribbean coral reefs. Mar Biol 141:387-400
LaJeunesse TC, Trench RK (2000) Biogeography of two species of *Symbiodinium* (Freudenthal) inhabiting the intertidal sea anemone *Anthopleura elegantissima* (Brandt). Biol Bull 199:126-134
Lasker HR (1981) A comparison of the particulate feeding abilities of three species of gorgonian soft coral. Mar Ecol Prog Ser 5:61-67
Lasker HR (1985) Prey preferences and browsing pressure of the butterflyfish *Chaetodon capistratus* on Caribbean gorgonians. Mar Ecol Prog Ser 21:213-220
Lasker HR (2005) Gorgonian mortality during a thermal event in the Bahamas. Bull Mar Sci

76:155-162
Lasker HR, Peters EC, Coffroth MA (1984) Bleaching of reef coelenterates in the San Blas Islands, Panama. Coral Reefs 3:183-190
Lasker HR, Coffroth MA, Fitzgerald LM (1988) Foraging patterns of *Cyphoma gibbosum* on octocorals: the roles of host choice and feeding preference. Biol Bull 174:254-266
Lasker HR, Boller ML, Castanaro J, Sánchez JA (2003) Determinate growth and modularity in a gorgonian octocoral. Biol Bull 205:319-330
Lesser MP, Shick JM (1989) Effects of irradiance and ultraviolet radiation on photoadaptation in the zooxanthellae of *Aiptasia pallida*: primary production, photoinhibition, and enzymic defenses against oxygen toxicity Mar Biol 243-255
Lesser MP, Stochaj WR, Tapley DW, Shick JM (1990) Bleaching in coral reef anthozoans: effects of irradiance, ultraviolet radiation, and temperature on the activities of protective enzymes against active oxygen. Coral Reefs 8:225-232
Lewis JB, Post EE (1982) Respiration and energetics in West Indian Gorgonacea (Anthozoa, Octocorallia). Comp Biochem Physiol A Comp Physiol 71:457-459
Loya Y, Sakai K, Yamazato K, Nakano Y, Sambali H, van Woesik R (2001) Coral bleaching: the winners and the losers. Ecol Lett 4:122-131
Marsh JJA (1970) Primary productivity of reef-building calcareous red algae. Ecology 51:255-263
Mergner H, Svoboda A (1977) Productivity and seasonal changes in selected reef areas in the Gulf of Aqaba (Red Sea). Helgoländer wiss Meeresunters 30:383-399
Middlebrook R, Hoegh-Guldberg O, Leggat W (2008) The effect of thermal history on the susceptibility of reef-building corals to thermal stress. J Exp Biol 211:1050-1056
Miller SL, Chiappone M, Rutten LM (2009) Large-scale assessment of the abundance, distribution, and condition of benthic coral reef organisms in the Florida Keys National Marine Sanctuary - 2009 Quick look report and data summary. CMS/UNCW, Key Largo FL
Murdock GR (1978a) Digestion, assimilation, and transport of food in the gastrovascular cavity of a gorgonian octocoral (Cnidaria; Anthozoa). Bull Mar Sci 28:354-362
Murdock GR (1978b) Circulation and digestion of food in the gastrovascular system of gorgonian octocorals (Cnidaria; Anthozoa). Bull Mar Sci 28:363-370
Muscatine L (1967) Glycerol excretion by symbiotic algae from corals and *Tridacna* and its control by the host. Science 156:516-519
Muscatine L, Cernichiari E (1969) Assimilation of photosynthetic products of zooxanthellae by a reef coral. Biol Bull 137:506-523
Muscatine L, Falkowski PG, Porter JW, Dubinsky Z (1984) Fate of photosynthetic fixed carbon in light- and shade-adapted colonies of the symbiotic coral *Stylophora pistillata*. Proc R Soc Biol Sci Ser B 222:181-202
Mydlarz LD, Jacobs RS (2006) An inducible release of reactive oxygen radicals in four species of gorgonian corals. Mar Freshw Behav Phy 39:143-152
Odum HT, Odum EP (1955) Trophic structure and productivity of a windward coral reef community on Eniwetok Atoll. Ecol Monogr 25:291-320

Padilla-Gamiño JL, Pochon X, Bird CE, Concepcion GT, Gates RD (2012) From parent to gamete: vertical transmission of *Symbiodinium* (Dinophyceae) ITS2 sequence assemblages in the reef building coral *Montipora capitata*. PLoS ONE 7:e38440

Pallas PS (1766) Elenchus zoophytorum sistens generum adumbrationes generaliores et specierum cognitarum succinctas descriptiones cum selectis auctorum synonymis. Hagae Comitum:451

Pandolfi JM, Jackson JBC, Baron N, Bradbury RH, Guzman HM, Hughes TP, Kappel CV, Micheli F, Ogden JC, Possingham HP, Sala E (2005) Are U.S. coral reefs on the slippery slope to slime? Science 307:1725-1726

Pettay DT, LaJeunesse TC (2007) Microsatellites from clade B *Symbiodinium* spp. specialized for Caribbean corals in the genus *Madracis*. Mol Ecol Notes 7:1271-1274

Pinzon JH, LaJeunesse TC (2011) Species delimitation of common reef corals in the genus *Pocillopora* using nucleotide sequence phylogenies, population genetics and symbiosis ecology. Mol Ecol 20:311-325

Platt T, Gallegos CL, Harrison WG (1980) Photoinhibition of photosynthesis in natural assemblages of marine phytoplankton. J Mar Res 38:687-701

Pochon X, Gates RD (2010) A new *Symbiodinium* clade (Dinophyceae) from soritid foraminifera in Hawai'i. Mol Phylogen Evol 56:492-497

Poland DM, Mansfield JM, Hannes AR, Lewis CLF, Shearer TL, Connelly SJ, Kirk NL, Coffroth MA (2013) Variation in *Symbiodinium* communities in juvenile *Briareum asbestinum* (Cnidaria: Octocorallia) over temporal and spatial scales. Mar Ecol Prog Ser 476:23-37

Posada D (2008) jModelTest: phylogenetic model averaging. Mol Biol Evol 25:1253-1256

Posada D (2009) Selection of models of DNA evolution with jModelTest. Methods in molecular biology (Clifton, NJ) 537:93-112

Prada C, Hellberg ME (2013) Long prereproductive selection and divergence by depth in a Caribbean candelabrum coral. Proc Natl Acad Sci U S A 110:3961-3966

Prada C, Schizas NV, Yoshioka PM (2008) Phenotypic plasticity or speciation? A case from a clonal marine organism. BMC Evol Biol 8:47

Prada C, Weil E, Yoshioka PM (2010) Octocoral bleaching during unusual thermal stress. Coral Reefs 29:41-45

Ramus J, Beale SI, Mauzerall D (1976) Correlation of changes in pigment content with photosynthetic capacity of seaweeds as a function of water depth. Mar Biol 37:231-238

Ribes M, Coma R, Gili J-M (1998) Heterotrophic feeding by gorgonian corals with symbiotic zooxanthella. Limnol Oceanogr 43:1170-1179

Rodríguez AD (1995) The natural products chemistry of West Indian gorgonian octocorals. Tetrahedron 51:4751-4618

Rodríguez-Martínez RE, Ruíz-Rentería F, van Tussenbroek B, Barba-Santos G, Escalante-Mancera E, Jordán-Garza G, Jordán-Dahlgren E (2010) Environmental state and tendencies of the Puerto Morelos CARICOMP site, Mexico. Rev Biol Trop 58 Suppl 3:23-43

Rodríguez-Román A, Hernandez-Pech X, Thomé PE, Enríquez S, Iglesias-Prieto R (2006)

Photosynthesis and light utilization in the Caribbean coral *Montastraea faveolata* recovering from a bleaching event. Limnol Oceanogr 51:2702-2710
Rowan R (2004) Coral bleaching: thermal adaptation in reef coral symbionts. Nature 430:742
Ruzicka RR, Colella MA, Porter JW, Morrison JM, Kidney JA, Brinkhuis V, Lunz KS, Macaulay KA, Bartlett LA, Meyers MK, Colee J (2013) Temporal changes in benthic assemblages on Florida Keys reefs 11 years after the 1997/1998 El Niño. Mar Ecol Prog Ser 489:125-141
Sampayo EM, Franceschinis L, Hoegh-Guldberg O, Dove SG (2007) Niche partitioning of closely related symbiotic dinoflagellates. Mol Ecol 16:3721-3733
Sampayo EM, Ridgway T, Bongaerts P, Hoegh-Guldberg O (2008) Bleaching susceptibility and mortality of corals are determined by fine-scale differences in symbiont type. Proc Natl Acad Sci U S A 105:10444-10449
Sánchez JA, Cairns S (2004) An unusual new gorgonian coral (Anthozoa: Octocorallia) from the Aleutian Islands, Alaska. Zool Meded 78:265-274
Sánchez JA, Wirshing HH (2005) A field key to the identification of tropical western Atlantic zooxanthellate octocorals (Octocorallia: Cnidaria). Carib J Sci 41:508-522
Sánchez JA, Mcfadden CS, France SC, Lasker HR (2003) Molecular phylogenetic analyses of shallow-water Caribbean octocorals Mar Biol 975-987
Santos SR, Taylor DJ, Coffroth MA (2001) Genetic comparisons of freshly isolated vs. cultured symbiotic dinoflagellates: implications for extrapolating to the intact symbiosis. J Phycol 37:900-912
Santos SR, Shearer TL, Hannes AR, Coffroth MA (2004) Fine-scale diversity and specificity in the most prevalent lineage of symbiotic dinoflagellates (*Symbiodinium*, Dinophyceae) of the Caribbean. Mol Ecol 13:459-469
Sebens KP (1984) Water flow and coral colony size: interhabitat comparisons of the octocoral *Alcyonium siderium*. Proc Natl Acad Sci U S A 81:5473-5477
Seibt C, Schlichter D (2001) Compatible intracellular ion composition of the host improves carbon assimilation by zooxanthellae in mutualistic symbioses. Naturwissenschaften 88:382-386
Sutton DC, Hoegh-Guldberg O (1990) Host-zooxanthella interactions in four temperate marine invertebrate symbioses: assessment of effect of host extracts on symbionts. Biol Bull 178:175-186
Tchernov D, Gorbunov MY, de Vargas C, Narayan Yadav S, Milligan AJ, Häggblom M, Falkowski PG (2004) Membrane lipids of symbiotic algae are diagnostic of sensitivity to thermal bleaching in corals. Proc Natl Acad Sci U S A 101:13531-13535
Thompson PA, Harrison PJ, Parslow JS (1991) Influence of irradiance on cell volume and carbon quota for ten species of marine phytoplankton J Phycol. Blackwell Science Inc 351-360
Thornhill DJ, Kemp DW, Bruns BU, Fitt WK, Schmidt GW (2008) Correspondence between cold tolerance and temperate biogeography in a western atlantic *Symbiodinium* (Dinophyta) lineage. J Phycol 44:1126-1135
Thornhill DJ, Xiang Y, Pettay DT, Zhong M, Santos SR (2013) Population genetic data of a

model symbiotic cnidarian system reveal remarkable symbiotic specificity and vectored introductions across ocean basins. Mol Ecol 22:4499-4515
Todd PA (2008) Morphological plasticity in scleractinian corals. Biol Rev 83:315-337
Tunn KPP, Chou LM, Cheshire AC (1996) Photophysiological studies of the soft coral *Sinularia* in the turbid waters of Singapore. The Marine Biology of the South China Sea III: Proceedings of the Third International Conference on the Marine Biology of the South China Sea:275
van Woesik R, Sakai K, Ganase A, Loya Y (2011) Revisiting the winners and the losers a decade after coral bleaching. Mar Ecol Prog Ser 434:67-76
van Woesik R, Irikawa A, Anzai R, Nakamura T (2012) Effects of coral colony morphologies on mass transfer and susceptibility to thermal stress. Coral Reefs 31:633-639
Veron JEN, Stafford-Smith M (2000) Corals of the World. Australian Institute of Marine Science
Vreeland HV, Lasker HR (1989) Selective feeding of the polychaete *Hermodice carunculata* Pallas on Caribbean gorgonians. J Exp Mar Bio Ecol 129:265-277
Wang JT, Meng P-J, Sampayo EM, Tang SL, Chen CA (2011) Photosystem II breakdown induced by reactive oxygen species in freshly-isolated *Symbiodinium* from *Montipora* (Scleractinia; Acroporidae). Mar Ecol Prog Ser 422:51-62
Warner ME, Berry-Lowe S (2006) Differential xanthophyll cycling and photochemical activity in symbiotic dinoflagellates in multiple locations of three species of Caribbean coral. J Exp Mar Bio Ecol 339:86-95
Warner ME, Fitt WK, Schmidt GW (1999) Damage to photosystem II in symbiotic dinoflagellates: A determinant of coral bleaching. Proc Natl Acad Sci U S A 96:8007-8012
Warner ME, Lesser MP, Ralph PJ (2010) Chlorophyll fluorescence in reef building corals. In: Suggett DJ, Prášil O, Borowitzka MA (eds) Chlorophyll *a* Fluorescence in Aquatic Sciences: Methods and Applications. Springer Netherlands, Dordrecht, pp209-222
Weis VM (2008) Cellular mechanisms of Cnidarian bleaching: stress causes the collapse of symbiosis. J Exp Biol 211:3059-3066
West JM, Harvell CD, Walls AM (1993) Morphological plasticity in a gorgonian coral (*Briareum asbestinum*) over a depth cline. Mar Ecol Prog Ser 94:61-69
Yellowlees D, Rees TAV, Leggat W (2008) Metabolic interactions between algal symbionts and invertebrate hosts. Plant Cell Environ 31:679-694
Zwickl DJ (2006) Genetic algorithm approaches for the phylogenetic analysis of large
biological sequence datasets under the maximum likelihood criterion. The University of Texas at Austin

VITA

Blake Ramsby
Department of Biology, University of Mississippi
526 Shoemaker Hall
University, MS 38677
Phone: (407) 739 5802
blake.ramsby@gmail.com

EDUCATION

Bachelor of Science in Biology — 2008
Bachelor of Science in Environmental Studies
University of Richmond, Richmond, VA, USA

TEACHING

Biology Department tutor — 2013

Teaching assistant (BISC103, BISC105, BISC161, BISC163) — 2009-2013

GRANTS RECEIVED

"Associating algal response to temperature stress with its genetic identity". The Explorer's Club. $1000 — 2012

"Physiology of octocoral symbionts under elevated temperatures". University of Mississippi Graduate Student Research Program. $495 — 2009

PUBLICATIONS

Ramsby, B., Iglesias-Prieto, R., & Goulet, T. L. Symbiosis and host morphological variation: *Symbiodinium* photosynthesis in the octocoral *Briareum asbestinum* at ambient and elevated temperatures — *submitted*

Ramsby, B., Shirur, K., Iglesias-Prieto, R., & Goulet, T. L. *Symbiodinium* photosynthesis in Caribbean octocorals. — *submitted*

Ramsby, B., Massaro M., Marshall, E., Wilcox, T., & Malcolm Hill. Epibiont–basibiont interactions: examination of ecological factors that influence specialization in a two-sponge association between *Geodia vosmaeri* (Sollas, 1886) and *Amphimedon erina* (de Laubenfels, 1936). *Hydrobiologia*, pp. 1-10, doi:10.1007/s10750-011-0878-y. 2012

Hill, M., Allenby A., Ramsby, B., Schönberg, C., & April Hill. *Symbiodinium* diversity among host clionaid sponges from Caribbean and Pacific reefs: Evidence of heteroplasmy and putative host-specific symbiont lineages. *Molecular Phylogenetics and Evolution* 59: 81-88. 2011

Weisz, J., Massaro, A., Ramsby, B. & Malcolm Hill. Zooxanthellar symbionts shape host sponge trophic status through translocation of carbon. *Biological Bulletin* 219: 189–197. 2010

PRESENTATIONS

Benthic Ecology Meeting; Norfolk, VA 2012
The photophysiology of clade B *Symbiodinium* in Caribbean gorgonians (talk)

University of Mississippi research symposium 2011
Octocoral symbionts tolerate thermal stress

Society of Integrative and Comparative Biology; San Antonio, Texas 2008
Zooxanthellar symbionts of the Clionaidae: A case study involving the *Cliona varians* species complex (poster)

University of Richmond Undergraduate Research Symposium (posters) 2008
(1) Examining zooxanthellae from the different forms of *Cliona varians*
(2) DGGE analysis of species-specific decompositional fungi